Author/s:
Nadurata, VL;Boskovic, C

Title:
Switching metal complexes via intramolecular electron transfer: connections with solvatochromism

Date:
2021-04-07

Citation:
Nadurata, V. L. & Boskovic, C. (2021). Switching metal complexes via intramolecular electron transfer: connections with solvatochromism. INORGANIC CHEMISTRY FRONTIERS, 8 (7), pp.1840-1864. https://doi.org/10.1039/d0qi01490g.

Persistent Link:
https://hdl.handle.net/11343/333723

Switching metal complexes via intramolecular electron transfer: connections with solvatochromism

Vincent L. Nadurata and Colette Boskovic

School of Chemistry, University of Melbourne, Parkville, Victoria, 3010, Australia

E-mail: c.boskovic@unimelb,edu,au

Abstract

Metal complexes that can exist in two different charge distributions often exhibit dramatic color changes when switched between them. The underlying spectral changes are fundamentally related to the switchable behavior. In valence tautomeric (VT) systems, the transition is a stimulated, reversible intramolecular electron transfer between a metal center and a ligand, while in so-called charge-transfer-induced spin transition (CTIST) systems, also known as electron-transfer-coupled-spin-transition (ETCST), the electron is transferred between two metal centers. We discuss, herein, the relationships between the switchable behavior of these systems and two related optical phenomena: charge transfer and solvatochromism. The insights gained from analyzing these phenomena can illuminate important aspects of VT or CTIST behavior, for example, the energetic relationship between the electromeric forms, or the effects of molecular environment on a VT or CTIST thermal equilibrium. Such insights may assist efforts to employ these compounds as molecular scale components in data storage, sensor and display devices.

Introduction

In recent years, switchable phenomena have become increasingly sought-after in molecular materials. The ability to reversibly switch between two or more states, aside from being fascinating from a fundamental chemistry perspective, is an important feature for practical applications in sensing, displays, molecular electronics, and in particular, data storage.[1–4] While the miniaturization of silicon-based components faces major obstacles – superparamagnetism, quantum effects, and heat, for example[4–6] – switchable molecules offer the potential to store data at the molecular scale, or serve as individual electronic or spintronic components in a device. Meanwhile, the vivid color changes that often accompany the transition between states lend these systems the potential for use as molecular scale components in chromic-based sensors and displays.

In coordination chemistry, the richly variable and practically limitless store of combinations of metals and ligands allows the tailoring of a molecule's properties toward various switchable behaviors; it is possible to switch a molecule's architecture, magnetic moment, spin state, and charge distribution.[7–10] This review is concerned with the last of these categories.

If a redox-active metal is bound to a redox-active ligand, it may be possible to observe two different charge distributions, as shown in Fig. 1. The process of reversibly switching between one charge distribution and another via application of an external stimulus is known as valence tautomerism (VT).[11,12] The interconversion corresponds to a transfer of charge between metal and ligand. The language used here is suggestive – the process is related to that which proceeds in a metal-to-ligand or ligand-to-metal charge transfer excitation. Although there are many differences between VT and optical charge transfer, since the two processes are concerned with the same two redox configurations (Fig. 1) it is possible to draw relationships between them. Charge transfer excitations often exhibit strong, readily observable bands in the UV-vis-NIR region, and so, analysis of a compound's charge transfer spectra can provide useful insight into its valence tautomeric behavior.[13,14]

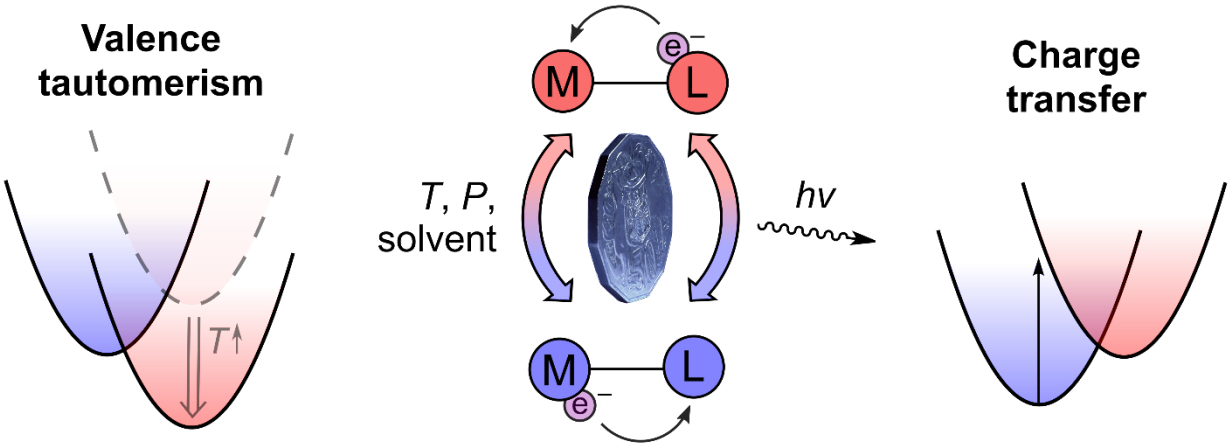

Fig. 1 Valence tautomeric transitions and charge transfer excitations are two sides of the same coin.

Compounds with prominent charge transfer spectra often exhibit solvent dependence of the electronic spectrum, also known as solvatochromism.[15–18] While d-d and ligand-centered transitions can manifest this phenomenon, it is more common for charge transfer transitions, since these are often associated with a large reorganization energy and significant change in dipole moment – both of these effects lend themselves to solvent dependence, for reasons discussed below.[19,20]

Solvatochromism arises when the stabilization of the ground state relative to the excited state differs between different solvents.[21] The ground and excited states in a charge transfer transition are redox isomers. Accordingly, the solvatochromism of charge transfer bands not only reports on changes in the energy separation between ground and excited states, but also, and equivalently, on changes in the energy separation between redox isomers, and potentially, in some cases, on the position of a VT equilibrium.[22,23] Considerable theory has been developed to treat solvatochromism in metal complexes; there are numerous parameters that describe the various solvent-solute interactions that may contribute to solvatochromism.[21,24–27] We will demonstrate below the use of solvatochromic theory to interpret solvent effects on VT equilibria.

The first section of this review discusses the theories of optical charge transfer and solvatochromism, and their relationship to redox-switchable molecules, first connecting VT with charge transfer, then connecting charge transfer with solvatochromism. The second section expands on the connections between VT and charge transfer. We survey the

response of charge transfer spectra to ligand tuning and other effects, and its implications for redox isomerism, a category which, aside from VT, additionally includes charge-transfer-induced spin transition (CTIST), also known as electron-transfer-coupled spin transition (ETCST), a closely related phenomenon involving charge transfer between two metal centers.

The latter part of this review addresses solvatochromism, beginning with a discussion of the solvatochromic behavior of some non-valence tautomeric complexes. These examples illustrate some of the varying solvent-solute interactions that can cause solvatochromism, as well as the rich variety of solvatochromic behaviors exhibited by cobalt complexes. In general, throughout the review, we concentrate mainly on cobalt complexes, due to this metal's numerous advantages in switchability applications. Our focus then moves to complexes exhibiting both VT and solvatochromism. In certain cases, the position of a VT equilibrium can be manipulated by choice of solvent. While it is well known that changes in the molecular environment in the crystalline phase can have significant ramifications for VT behavior,[28–30] environmental effects on VT in solution have not been discussed in detail. Accordingly, understanding the solvent-solute interactions that underlie this behavior is of key importance. We then present a survey of solvent dependent VT, using solvatochromic arguments developed in the theory section to suggest various explanations for the effects of solvent on the position of VT equilibria.

Due to the dramatic color responses that solvatochromic compounds sometimes exhibit, they have the potential for applications as sensors and indicators.[20,31] The sensing behaviors of a few solvatochromic cobalt compounds are briefly discussed.

Theories of charge transfer and solvatochromism from the perspective of switchable molecules

Charge transfer is one of the most fundamental phenomena in all of chemistry, underpinning a variety of light driven processes from such wide-ranging areas as photosynthesis, photocatalysis, and photovoltaics.[32–34] In the majority of cases, the transition between ground D-A (D = donor, A = acceptor) and excited D^+-A^- states is mediated by light absorption. Marcus theory (Fig. 2) relates the optical excitation energy (E_{op}) to the reorganizational energy (λ) and the energy difference between the lowest vibrational levels of the ground and excited states (ΔG_0) via

$$E_{op} = \Delta G_0 + \lambda, \quad (1)$$

where λ can alternatively be expressed as the sum of the vibrational (λ_v) and solvent (λ_o) reorganizational energies.[19]

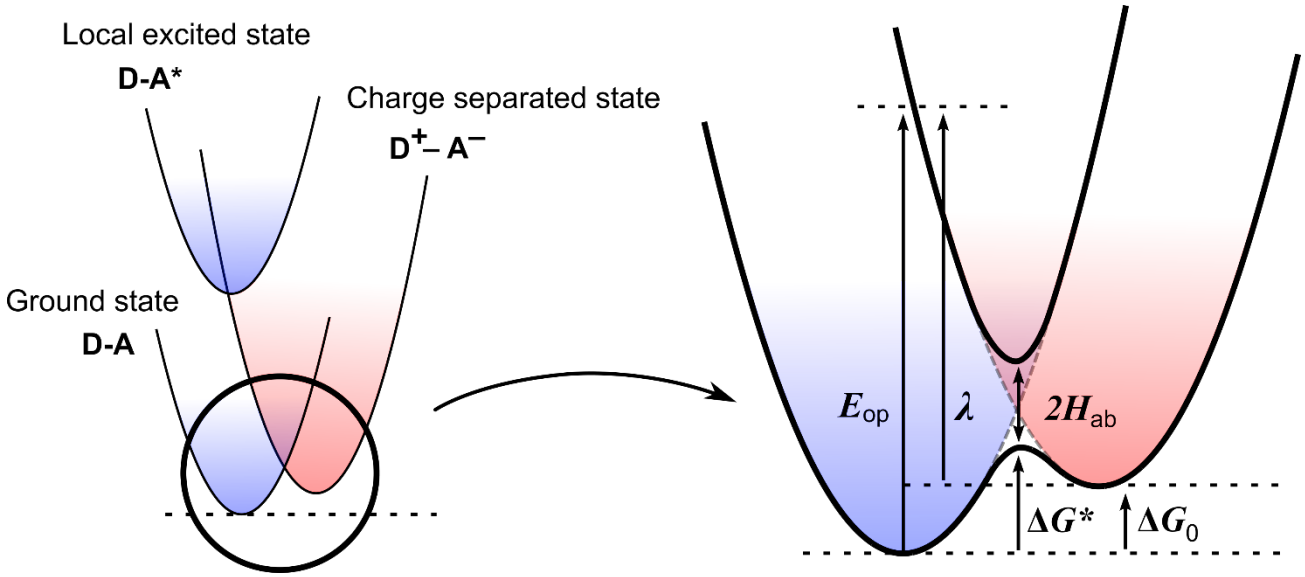

Fig. 2 The relationship between charge transfer parameters for a general donor-acceptor pair.[19] E_{op} is the energy of the optical excitation energy, λ is the reorganizational energy, H_{ab} is the electronic coupling parameter, ΔG^* is the activation energy, and ΔG_0 is the zero-level energy difference between ground and excited states. The potential energy surfaces are described by equations that may be found in Ref. [35].

At low temperatures, the photoinduced D^+-A^- excited state can, in certain cases, be long-lived.[30,36] For example, irradiation at low temperatures of the LMCT bands of some cobalt-catecholate systems results in evolution to metastable D^+-A^- states, which can have relaxation times, τ, on the order of 10^5 or 10^6 s.[29,37] This effect is generally known as light-induced excited spin-state trapping (LIESST), and in VT systems can more specifically be called light induced VT (LIVT). It can also be observed closer to room temperature in solution via transient absorption spectroscopy, albeit with drastically reduced relaxation times.[38] The utility of such studies in elucidating mechanistic details of the optically induced VT process will be expanded upon in the next section. The LIESST effect is also observed in many Co-Fe Prussian blue analogues,[39,40] with one such example exhibiting a relaxation time, at 120 K, of about 10 years.[41]

Alternatively, there are cases where the transition between D-A and D^+-A^- states is thermally driven. In metal-ligand D-A systems, this is also known as thermally-induced VT.[11]

The archetypal VT complex $[Co(diox)_2(bipy)]^+$ (diox = 3,5-di-*tert*-butyl-dioxolene, bipy = 2,2′-bipyridine) is present as the low spin cobalt(III) catecholate (LS-Co^{III}-cat) tautomer (effectively the D-A state) at low temperatures, whereas at high temperatures it is present as the high spin cobalt(II) semiquinonate (HS-Co^{II}-sq) tautomer (effectively the D^+-A^- state).[42] The transition is entropically driven. The higher entropy of the HS-Co^{II}-sq tautomer, arising from longer metal-ligand bond lengths and an increased spin degeneracy compared to the LS-Co^{III}-cat form, is responsible for the thermodynamic preference of the system to adopt a semiquinonate-Co^{II} redox configuration at high temperatures. Within a two-state model, thermally induced VT constitutes a temperature dependent reversal of the energies of the D-A and D^+-A^- states, so that the D^+-A^- state is thermodynamically preferred at high temperatures (Fig. 1, left). For cobalt VT systems, the situation is more complicated. The high temperature tautomer is not the same as the D^+-A^- excited state, due to a spin state change at the metal center that accompanies the thermal transition.[13] The exact nature of the D^+-A^- excited state can be probed with transient spectroscopy..

Valence tautomerism is only one possibility amongst a variety of behaviors that may be exhibited by a D-A pair. While in VT systems, the charge distribution in an individual molecule can be unambiguously assigned, for a general D-A pair, there are two limiting cases: one involving fully localized redox states, and the other involved fully delocalized redox states. The variety of behaviors exhibited within this continuum is illustrated in Fig. 3. In the upper row (a, b, and c) are compounds wherein the donor and acceptor units are the same element – these constitute examples of mixed-valency under Robin and Day's original classification.[43] Class II mixed-valence compounds exhibit charge localization **(a)**, Class III mixed-valence compounds exhibit charge delocalization **(c)**, and Class II-III mixed-valency is an intermediate case **(b)**.[44] In contrast, the compounds in the lower row **(e, f, and g)** are not mixed-valent compounds under Robin and Day's original classification; the donor and acceptor units are not the same element. In each, the donor unit is a metal, but in **(e)** and **(f)**, the acceptor unit is a ligand, and in **(g)**, the acceptor unit is a different metal.[42,45,46] However, since they lie on the redox localized side of the continuum, the interaction between donor and acceptor units in these systems can be likened to Class II mixed-valency.

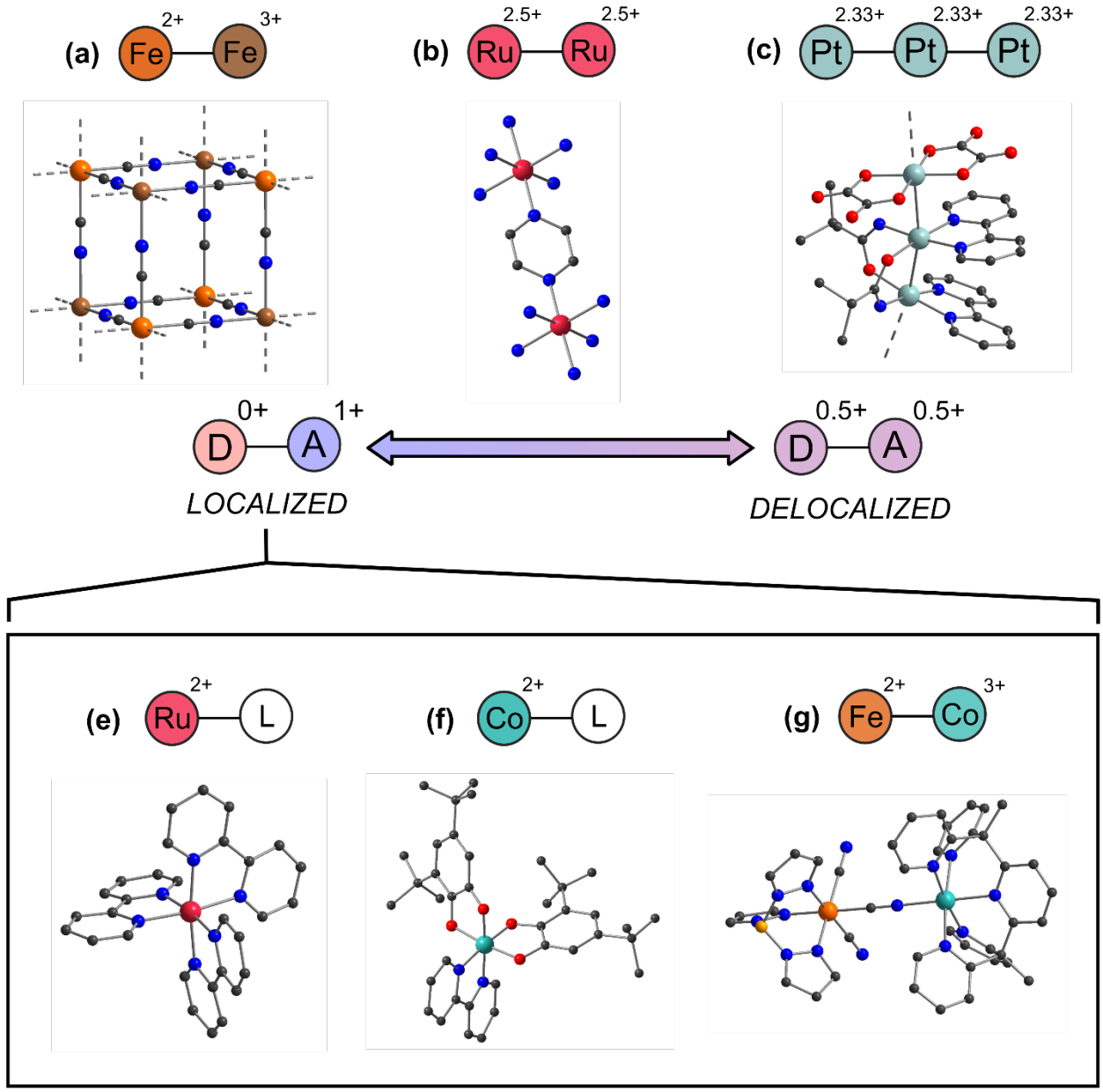

Fig. 3 Varying behaviors exhibited by donor-acceptor pairs in inorganic complexes. Prussian blue **(a)** is a class II mixed-valence compound with distinct Fe^{II}/Fe^{III} and Fe^{III}/Fe^{II} states.[47] This is in contrast to the class III mixed-valent 1D Pt chain $\{[Pt_2(bipy)_2(\mu\text{-pivalamidate})_2][Pt(oxalate)_2]\}^+$ **(c)**, in which one positive charge per three Pt^{II} ions is equally distributed among them.[48] The Creutz-Taube ion **(b)** is an intermediate case (class II-III).[49,50] Within the class of localized valences it is possible to observe conventional charge transfer behavior, as in $[Ru(bipy)_3]^{2+}$ **(e)**; valence tautomerism, as in $[Co(diox)_2(bipy)]^+$ **(f)**; or CTIST, as in $\{[Fe(Tp)(CN)_3][Co(L)]\}^+$ (Tp = hydrotris(pyrazol-1-yl)borate, L = 2,6-bis(1,1-bis(2-pyridyl)ethyl)pyridine) **(g)**.[42,45,46]

Delocalization of charge occurs when the activation energy ΔG^* is low enough that the D^+-A^- state can be intermixed with the D-A state. Small values of the electronic coupling parameter, H_{ab}, lead the system to a double well potential (Fig. 2), within which the D-A and

D^+-A^- states carry distinct identities, whereas large values of H_{ab} contribute to a mixing of the two states and increased delocalization of charge. In both cases, charge transfer bands are frequently observed in the optical spectra. These bands have been studied extensively in mixed-valence systems, in which the excitation is more commonly labelled using the term intervalence charge transfer (IVCT).[44,51,52] Hence, in the following, we focus on cases involving different donor and acceptor units, namely, charge transfer between a metal and a ligand – metal-to-ligand (MLCT) or ligand-to-metal charge transfer (LMCT) – or between two different metals – metal-to-metal charge transfer (MMCT).

One of the hallmarks of a charge transfer transition is the phenomenon of solvatochromism – the solvent dependence of a compound's electronic spectrum.[21,53] Although not all solvatochromic transitions are charge transfer transitions, and not all charge transfer transitions are solvatochromic,[51] charge transfer transitions are, by their nature, particularly susceptible to solvent dependence. Due to the large change in dipole moment that can often accompany charge transfer, the ground and excited states may be stabilized to different extents by the dielectric properties of the solvent, causing λ_o and therefore E_{op} to vary between solvents. If E_{op} is in the visible region, this behavior is phenomenologically observed as a change in color between different solvents.

Alternatively, solvatochromism can be caused by an equilibrium between two different species, where the ground state in fact changes between solvents, such as in the complexes $[Co(Me_3tpa)(Br_4diox)]^+$ (Me_3tpa = tris(6-methyl-2-pyridylmethyl)amine, Br_4diox = tetrabromodioxolene) and $[Fe^{II}(L)]^{2+}$ (L = *N*,*N′*-bis[(1,10-phenanthroline-2-yl)methyl]-cis-cyclohexane-1,2-diamine).[23,54] These two examples represent solvatochromism arising from solvent effects on, in the first case, a VT equilibrium, and in the second case, a SCO equilibrium. Solvent dependent VT equilibria will be discussed in detail further on. Since there are only a handful of detailed studies on solvent dependent SCO equilibria, this class of systems is not further discussed.[55–58]

We will first focus on solvatochromism arising from a change in excitation energy rather than a change in ground state. Fundamentally, this is caused by a solvent dependent variation in the stabilization of the ground state relative to the excited state. In most situations, this effect can be understood in terms of solvent polarity.[21] If the ground state has a larger dipole moment than the excited state, increasing the solvent polarity will result in a greater stabilization of the ground state compared to the excited state. Hence, the excitation energy will increase with solvent polarity. The MLCT transitions of the complex $[Ru^{II}(4,4'\text{-COOH-}2,2'\text{-bipyridine})_2(NCS)_2]$ exhibit such behavior, consistent with calculated ground and excited state

dipoles (in ethanol) of 19.81 and 9.56 D (1 D ≈ 3.34 x 10^{-30} C·m), respectively.[59] This is termed negative solvatochromism, while the opposite situation (a larger dipole moment in the excited state leading to a decrease in the excitation energy with increasing solvent polarity) is termed positive solvatochromism.

Within the context of inorganic molecules, the dipole rationalization for solvatochromism is very useful, due to the large changes in permanent dipole moment often associated with MLCT and LMCT transitions. In simple systems, such as in a series of tungsten(0) compounds $[W(CO)_5(L)]$ (L = various N-heteroaromatic ligands), dipole arguments can be applied on a qualitative basis.[60] The metal-ligand bond in the ground state is polarized as shown in Fig. 4a, due to the dominant σ donation from the ligand. Depending on the amount of electron density transferred as a result of the transition, the excited state can either have a smaller dipole **(i to iii)**, an equal and opposite dipole **(iv)**, or a larger dipole **(v)** compared to that in the ground state. Hence, as the acceptor strength of L increases, negative solvatochromism is initially observed, increasing to a maximum magnitude **(ii)**, then decreasing **(iii)**, before reaching zero **(iv)**, with positive solvatochromic behavior observed only if L is an exceptionally strong acceptor.[60] The latter case is rare, but has been observed in a handful of cases, for example, in certain zerovalent molybdenum carbonyl complexes.[61,62]

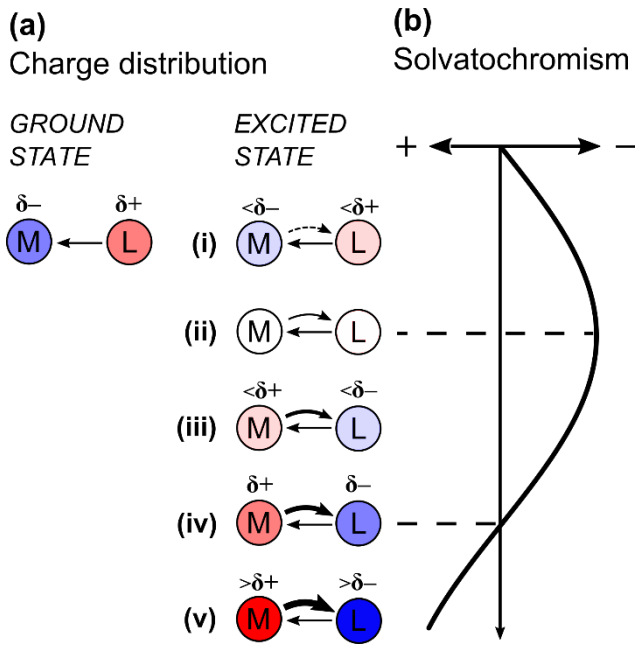

Fig. 4 An illustration of the dipole argument for rationalizing varying solvatochromic behaviors in $[W(CO)_5(L)]$.[60]

As outlined above, dipole arguments can provide a satisfactory explanation for the behavior of many solvatochromic complexes. However, there are also many cases where solvatochromism results not from the interactions between the molecular dipole and the solvent dielectric, but from other solvent-solute interactions, such as hydrogen bonding.[63]

To quantify solvatochromic behavior more generally it becomes necessary to also quantify solvent polarity and other solvent characteristics. Though physical constants such as the static dielectric constant (ε_r) and the refractive index (n) are sufficient in some cases,[17,64] excitation energies are most often plotted against an empirical parameter or functions thereof. Among the wide range of solvatochromic parameters are the Kamlet-Taft α- and β-parameters (which respectively measure hydrogen-bond donor and acceptor strength),[25] Gutmann's solvent donor and acceptor numbers (which respectively measure Lewis basicity and acidity),[24] and the Reichardt $E_T(30)$ parameter (which is derived from the energy of the solvatochromic π-π* transition in the organic dye 2,6-diphenyl-4-(2,4,6-triphenylpyridin-1-ium-1-yl)phenolate).[21] The most appropriate choice depends on the particular system, due to changes in the specific solvent-solute interactions from compound to compound. The $E_T(30)$ parameter, for example, exhibits an excellent linear correlation with the MLCT band energies across a range of complexes $[M(CO)_4(L)]$ (M = Cr, Mo, or W; L = 2,2′-bipyridine, 1,10-phenanthroline, 1,4-diazabutadiene, or substituted derivatives).[16]

Implications of charge transfer transitions for redox isomerism

In the following section, we expand on the connections between optical charge transfer and redox isomerism, focusing on complexes that exhibit redox isomerism, or those for which a redox isomeric transition may be theoretically envisaged. The latter category constitutes systems in which both donor and acceptor units are redox-active, with the oxidation of the donor and the reduction of the acceptor being each individually chemically reversible. A summary of these complexes is presented in Table 1, and their structures are illustrated in Fig. 5. We will discuss the response of their charge transfer spectra to ligand tuning or temperature variation, and the implications of these behaviors for redox isomerism.

Table 1 Energies of charge transfer transitions in selected complexes. When multiple charge transfer transitions are reported, only the lowest energy transition reported is listed. The structures are shown in Fig. 5.

Compound[a]	Number	Nature of transition[b]	Solvent	E_{op} (cm^{-1})	Redox isomerism	Ref.
[Fc-L_1-Ru(hfac)(P(*i*-Pr)$_3$)$_2$(CO)]$^+$	**1**	IET	DCE / 0.1 M Bu_4NPF_6	6,579	No	53
[Fc-L_1-Ru(acac)(P(*i*-Pr)$_3$)$_2$(CO)]$^+$	**2**	IET	DCE / 0.1 M Bu_4NPF_6	5,126	Yes	53
[$(CN)_5Fe^{II}(CN)Ru^{III}$(edta)]$^{5-}$	**3**	MMCT	Water	10,638	No	65
[Fc-CH_2=CH_2-PTM]	**4**	IET	*n*-hexane	11,223	Yes	19
[Me_8Fc-CH_2=CH_2-PTM]	**5**	IET	*n*-hexane	~7,700	Yes	66
[Co^{III}(cth)(Cl_4cat)]$^+$	**6**	LMCT	MeCN	14,793	No	13
[Co^{II}(pbqa)(*t*-Bu_2sq)]$^+$	**7**	MLCT	MeCN	17,391	Yes	67
[{Co(tpa)}$_2$(Br_4spiro)]$^{2+}$	**8**	LMCT	MeCN	14,387	No	14
[{Co(Me_2tpa)}$_2$(Br_4spiro)]$^{2+}$	**9**	LMCT	MeCN	12,361	Yes	14
[Co($L_2^{Me,Me}$)$_2$]$^{3+}$	**10**	LMCT	MeCN	11,628	No	68
[Co($L_2^{OMe,Me}$)$_2$]$^{3+}$	**11**	LMCT	MeCN	10,695	Yes	68
[Co(L_3^{Me})$_2$]$^{3+}$	**12**	LMCT	MeCN	13,106	No	69
[Co(L_3^{OMe})$_2$]$^{3+}$	**13**	LMCT	MeCN	11,751	No	69
[Co(*t*-Bu-salen)(OH_2)]$^+$	**14**	LMCT	DCM	9,434	No	70
[Co(MeO-salen)(OH_2)]$^+$	**15**	LMCT	DCM	8,197	No	70
{[(pzTp)Fe^{III}]$_4$$(CN)_{12}$[$Co^{II}$($Tp^{EtOH}$)]$_4$}$^{4+}$	**16**	MMCT	MeCN	19,608	Yes	41
{[(Tp*)(NC)Fe^{III}]$_2$$(CN)_4$[$Co^{II}$(*t*-Bu-bipy)]$_2$}$^{2+}$	**17**	MMCT	MeCN	17,857	Yes	71

[a] Abbreviations (in order mentioned): **Fc** = ferrocenyl, $\mathbf{L_1}$ = -C_6H_4-CH=CH-, **hfac**$^-$ = hexafluoroacetylacetonato, **DCE** = 1,2-dichloroethane, **acac**$^-$ = acetylacetonato, **edta**$^{4-}$ = ethylenediaminetetraacetate, **PTM** = perchlorotriphenylmethyl, **cth** = 5,7,7,12,14,14-hexamethyl-1,4,8,11-tetraazacyclotetradecane, $\mathbf{Cl_4cat^{2-}}$ = tetrachlorocatecholate, **pbqa** = (2-pyridylmethyl)bis(2-quinolylmethyl)amine, $\mathbf{t\text{-}Bu_2sq^-}$ = 3,5-tert-butylsemiquinonate, **tpa** = tris(2-pyridylmethyl)amine, $\mathbf{Br_4spiroH_4}$ = 3,3,3′,3′-tetramethyl-1,1′-spirobi(indan)-4,4′,7,7′-tetrabromo-5,5′,6,6′-tetraol, $\mathbf{Me_2tpa}$ = bis(6-methyl-2-pyridylmethyl)(2-pyridylmethyl)amine, $\mathbf{L_2}^{R,R'}$ = *N*-(4-*R*-phenyl)-*N*-(4-*R*′-phenyl)-6-(1,10-phenanthrolin-2-yl)pyridine-2-amine, $\mathbf{L_3}^{R}$ = *N,N*-bis(4-*R*-phenyl)-4′-phenyl-[2,2′:6′,2″-terpyridine]-6-amine, ***R*-salen** = *N,N*′-bis(3-tert-butyl-5-*R*-salicylidene)-1,2-cyclohexanediamine, **pzTp**$^-$ = tetra(pyrazol-1-yl)borate, $\mathbf{Tp^{EtOH}}$ = 2,2,2-tris(pyrazol-1-yl)ethanol, **Tp***$^-$ = hydrotris(3,5-dimethylpyrazol-1-yl)borate, **t-Bu-bipy** = 4,4′-di-tert-butyl-2,2′-bipyridine.

[b] Intramolecular electron transfer (IET).

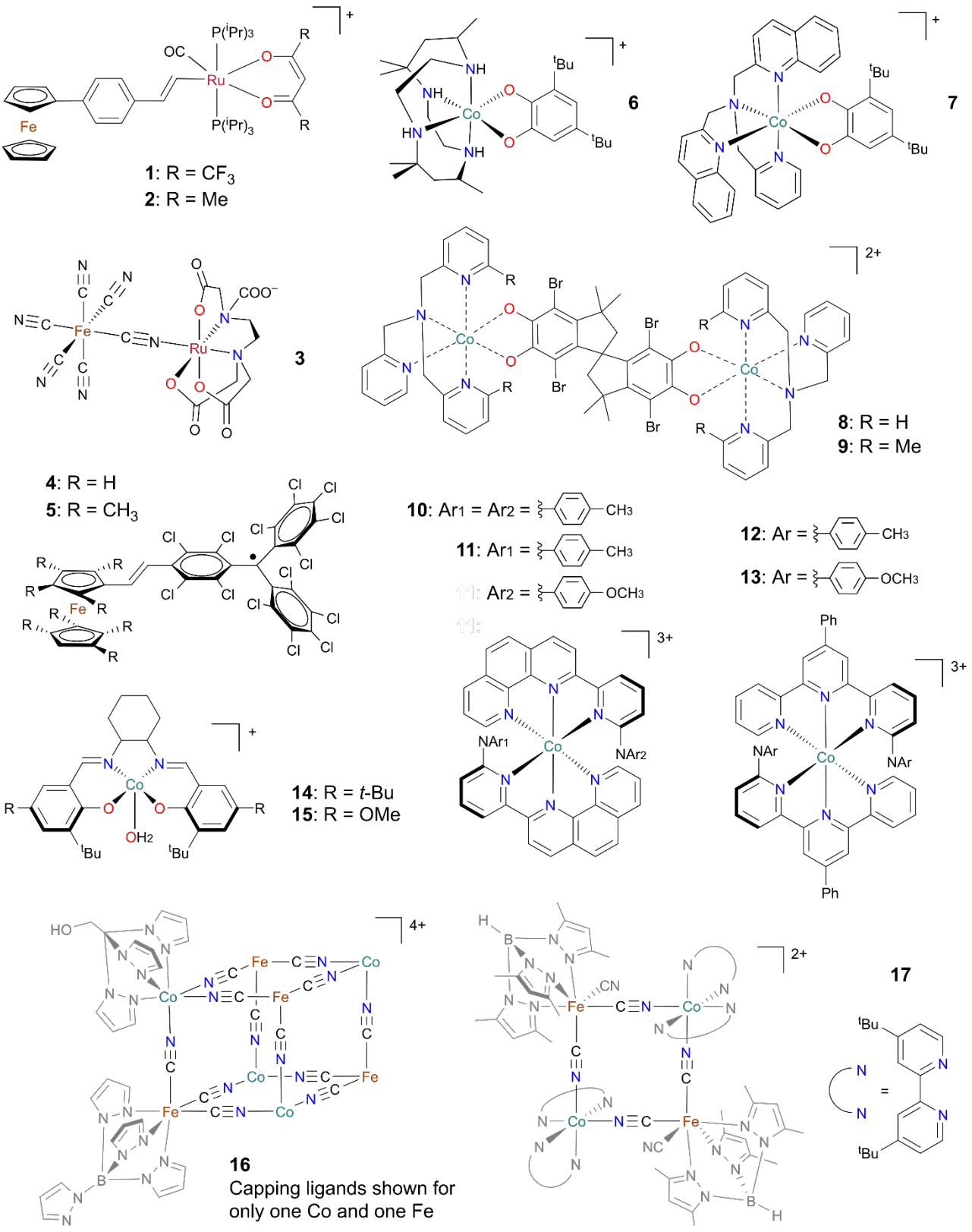

Fig. 5 Structures of complexes in Table 1.

The complexes [Fc-L_1-Ru(hfac)(P(*i*-Pr)$_3$)$_2$(CO)]$^+$ (**1**; Fc = ferrocenyl, L_1 = -C_6H_4-CH=CH-, hfac$^-$ = hexafluoroacetylacetonato) and [Fc-L_1-Ru(acac)(P(*i*-Pr)$_3$)$_2$(CO)]$^+$ (**2**; acac$^-$

= acetylacetonato) can potentially exist as two possible redox isomers – one with the positive charge on the ferrocenyl unit, represented as Fc^{+}-L_1-{Ru} [{Ru} = Ru(acac)(P(*i*-Pr)$_3$)$_2$(CO)], and the other with the positive charge delocalized over the styrylruthenium unit, represented as Fc-$[L_1$-{Ru}$]^{+}$.[53] For **1**, the highly electron withdrawing $hfac^{-}$ ligand causes the Fc-$[L_1$-{Ru}$]^{+}$ tautomer to be much higher in energy than the Fc^{+}-L_1-{Ru} tautomer, so that only the latter is present. Replacing $hfac^{-}$ with the more electron donating $acac^{-}$ ligand to give **2** lowers the energy of the Fc-$[L_1$-{Ru}$]^{+}$ tautomer enough that both redox isomers are present at room temperature, as evidenced by the splitting of the Ru(CO) infrared signal.

The shift of a near-IR band in moving from **1** to **2** gives an indication of this energy lowering. Since the band is assigned to an intramolecular electron transfer (IET) from the styrylruthenium unit to the ferrocenyl unit, the excited state of the transition is the same as the Fc-$[L_1$-{Ru}$]^{+}$ redox isomer. For **1**, the band appears at 6,579 cm^{-1}, while for **2**, it appears at 5,126 cm^{-1}, indicating that replacing $hfac^{-}$ with $acac^{-}$ lowers the energy difference between redox isomers by 1,453 cm^{-1}. Interestingly, using the positions of the first and second oxidations of the neutral complexes to estimate the same value gives a similar result – for **1**, $\Delta E_{1/2}$ is 452 mV while in **2** it is 280 mV, giving an energy lowering of 172 mV or 1,387 cm^{-1}. Noting that $\Delta G_0 \approx \Delta E_{1/2}$, these data indicate that in this system, ligand tuning has a minimal effect on λ [see eqn (1)]. In such systems, therefore, changes in E_{op} may be used to directly infer changes in ΔG_0.

The presence of a mixture of both redox isomers in solutions of **2** is a reflection of the relatively low energy of the styrylruthenium-to-ferrocenyl charge transfer. In comparison, the complex $[(CN)_5Fe^{II}(CN)Ru^{III}(edta)]^{5-}$ (**3**; $edta^{4-}$ = ethylenediaminetetraacetate), which also features iron and ruthenium centers, exhibits a much larger metal-to-metal charge transfer energy of 10,638 cm^{-1}. Accordingly, no redox isomeric equilibrium is observed.[65] Nevertheless, the thermochromism exhibited by **3**, characterized by thermally induced spectral changes, enables monitoring of the energy difference between Fe^{II}-Ru^{III} and Fe^{III}-Ru^{II} states. The linear dependence of E_{op} with temperature, with a gradient of -5 cm^{-1} K^{-1}, indicates that the energy difference between the two redox isomers decreases with increasing temperature – in other words, the Fe^{III}-Ru^{II} state is entropically favored. When the same trend is probed via electrochemistry, a very similar value of -6 cm^{-1} K^{-1} is obtained, demonstrating again that in such complexes as **1** to **3**, E_{op} and $\Delta E_{1/2}$ move in parallel. For the related compound $[(CN)_5Fe^{II}(CN)Ru^{III}(NH_3)_5]^{-}$ the same parallelism between E_{op} and $\Delta E_{1/2}$ is observed, albeit with a larger temperature dependence of -13.5 cm^{-1} K^{-1}. However, even at

high temperatures, the energy gap between the redox isomers remains too large to observe any equilibrium between them.[72]

Like **1** and **2**, the complexes [Fc-CH_2=CH_2-PTM] (**4**; PTM = perchlorotriphenylmethyl) and [Me_8Fc-CH_2=CH_2-PTM] (**5**) feature redox-active ferrocenyl units. Both exhibit intramolecular electron transfer (IET) bands in the near-IR region corresponding to charge transfer between the ferrocenyl donor unit and the perchlorotriphenylmethyl (PTM) acceptor unit. With a relatively high IET energy of 11,223 cm^{-1} (*n*-hexane), **4** is present purely in the neutral Fc-PTM state at room temperatue.[19] Methylation of the ferrocenyl unit to give **5** causes a lowering of the IET energy to around 7,700 cm^{-1} (*n*-hexane), corresponding to a decrease in the energy separation of the Fc-PTM ground and Fc^+-PTM^- excited states – which are also redox isomers. It is this decrease that gives rise to switchable behavior in **5**, which exhibits solvent induced VT – the Fc-PTM form is favored in non-polar solvents, and the Fc^+-PTM^- form in polar solvents. This effect can be interpreted as an extremely strong positive solvatochromism, whereby the Fc^+-PTM^- state is stabilized in polar solvents to such an extent that it becomes the ground state. In the crystalline phase, Mössbauer spectra at 295 K and 85 K reveal a thermally induced partial VT transition, revealing a Fe^{II}/Fe^{III} ratio of 88:12 at 85 K moving to 32:68 at 295 K.

The observation of VT behavior in both solution and crystalline phases, as observed in **5**, is not always guaranteed – in fact, there are numerous examples of VT observed in solution but not in the solid state, and vice versa.[42,73–75] The temperature range over which a solid state VT transition is observed may be inaccessible in solvent, and additionally, the solvent-solute interactions may be very different to the intermolecular interactions in the crystalline phase. For example, despite the lack of VT in solution samples of **4**, the species displays thermally induced VT in crystalline samples, as demonstrated by Mössbauer spectroscopy.[76]

Nevertheless, the solution-state charge transfer behavior of a donor-acceptor system can be used to predict switchable behavior in the crystalline phase. One treatment that achieves this uses a mean field Hamiltonian to model a crystal of donor-acceptor molecules.[77] The Hamiltonian incorporates the molecular parameters τ (the hybridization energy mixing the D-A and D^+-A^- states) and z (where $2z$ is the energy gap between D-A and D^+-A^- states), as well as a parameter pertaining to the crystal, the Madelung energy, M. It was proposed that for switchability, the relationship $z \approx -2M$ must be satisfied, and in addition, for bistability, the relationship $z/\tau > 1$ must also be satisfied. Bistability is a stronger claim than switchability,

requiring, in addition to two accessible states, the ability of the material to be found in both of these states under the same external conditions.[66]

In a study on **5**, *M* was calculated with quantum chemical calculations, while the molecular parameters *z* and τ were taken from the results of modelling the solution-state IET band.[66] The values obtained for the parameters were consistent with bistability in the crystalline phase. Similar work on **4** also gave values consistent with crystalline bistability, demonstrating the potential of the methodology to screen for bistability in the crystalline phase of neutral donor-acceptor molecules using charge transfer data from the solution phase.[78]

The remainder of the complexes listed in Table 1 feature cobalt centers. Cobalt is an attractive metal for use in switchable inorganic molecules due to the accessibility of both the di- and trivalent oxidation states, as well as the large entropy difference between low-spin Co^{III} and high-spin Co^{II}, which can facilitate thermal control of the system. For cobalt VT systems, the two-state donor-acceptor model gives an incomplete description of the charge transfer behavior. Studies on the complex $[Co^{III}(cth)(Cl_4cat)]^+$ (**6**; cth = 5,7,7,12,14,14-hexamethyl-1,4,8,11-tetraazacyclotetradecane, Cl_4cat^{2-} = tetrachlorocatecholate) have illustrated this. Ligand-to-metal charge transfer bands in the UV-vis spectrum were assigned based on their shift to lower energies upon replacement of tetrachlorocatecholate with 3,5-di-*tert*-butylcatecholate.[13] The study poses the question of whether the energies of these bands can be used to estimate ΔG_0. In this case, ΔG_0 is given by the difference in redox potentials of the Co^{III}-cat/Co^{II}-cat and Co^{II}-sq/Co^{II}-cat couples, where the former is determined experimentally and the latter is assumed to be the same as the redox potential of the Ni^{II}-sq/Ni^{II}-cat couple. This gives a value of 4,033 cm^{-1}, dramatically lower than the energy of the LMCT band, 14,518 cm^{-1}. Given eqn (1), this disparity is to be expected, since the LMCT excitation incorporates the additional energies of solvent reorganization as well as vibrational reorganization (see Fig. 2), which are particularly large in cobalt VT systems due to the significant difference in geometry between the two tautomers, with cobalt-ligand bond lengths changing by up to 0.2 Å.[79] In addition, the authors note a third cause for the disparity – while the electrochemical transition results in a HS-Co(II) species, the authors assign the LMCT transition as $3b_1$(catecholate) → e_g(Co), which would result not in a HS-Co(II) species but in a LS-Co(II) excited state.

A number of studies have attempted to spectroscopically assign the identity of the LMCT excited state in similar systems. Femtosecond resolved X-ray absorption near-edge structure (XANES) spectroscopy was used to show that LMCT excitation of a LS-Co^{III} complex

generates a LS-Co^{II} state, which proceeds, via intersystem crossing in 67 fs, to a HS-Co^{II} state that then relaxes via two pathways back to the ground state.[80] Likewise, transient IR spectroscopy was used to show that excitation of a certain LS-Co^{III}-cat complex at 810 nm generates an initial LMCT* state, which relaxes in under 200 fs to a metastable HS-Co^{II}-sq state.[81] Although the authors were unable to assign the LMCT* state as a LS-Co^{II}-sq species, the results, as in the previous example, indicate a two-step relaxation mechanism. Various electron paramagnetic resonance (EPR) studies on the LMCT excited states of similar systems are also consistent with two-step relaxation mechanisms.[82,83] In contrast, a density functional theory (DFT) study suggested that the thermal transition in the original $[Co(diox)_2(bipy)]^+$ VT compound occurs via a one-step mechanism, based on the calculated locations of the minimum energy crossing points (MECPs) on the potential energy surfaces of the system.[84] Altogether, these analyses point to there being fundamental differences between the mechanisms of optically and thermally induced VT in cobalt VT systems. As a result, the relationship between E_{op} and ΔG_0 is less direct than in more conventional donor-acceptor systems, namely, those for which the transition does not involve a spin-state change. In the case of **6**, this results in a large disparity between the values of E_{op} and ΔG_0.

Nevertheless, changes in E_{op} resulting from tuning the system or its environment may still give qualitative indications of interesting redox behavior. In the simplest cases, charge transfer bands can act as spectroscopic markers for a certain redox isomer. For example, the 575 nm MLCT band in $[Co^{II}(pbqa)(t\text{-}Bu_2sq)]^+$ (**7**; pbqa = (2-pyridylmethyl)bis(2-quinolylmethyl)amine, $t\text{-}Bu_2sq^-$ = 3,5-*tert*-butylsemiquinonate) indicates the presence of the HS-Co^{II}-sq tautomer, and its disappearance upon cooling is consistent with a transition to the LS-Co^{III}-cat tautomer.[67]

In more complicated cases, the trends in the energies of charge transfer bands in cobalt systems can still be related to trends in the relative stabilities of valence tautomers, similarly to the treatments of charge transfer spectra for complexes **1** to **5** above. The LMCT energies in toluene solution of a series of complexes $[Co(L)(3,6\text{-}t\text{-}Bu_2diox)_2]$ (L = a range of bidentate N donor ligands, 3,6-*t*-Bu_2diox = 3,6-di-*tert*-butyldioxolene) acts as a general guide for the position of the VT equilibrium at room temperature.[85] If the LMCT energy is greater than 4100 cm^{-1}, then the separation between HS-Co^{II}-sq and LS-Co^{III}-cat tautomers is large enough that the LS-Co^{III}-cat form is favored. On the other hand, of the complexes which favor the HS-Co^{II}-sq form at room temperature, those for which the LS-Co^{III}-cat tautomer is accessible via cooling all exhibit LMCT energies less than 4100 cm^{-1}.

A similar trend can be observed for the complexes $[\{Co(tpa)\}_2(Br_4spiro)]^{2+}$ (**8**; tpa = tris(2-pyridylmethyl)amine, $Br_4spiroH_4$ = 3,3,3′,3′-tetramethyl-1,1′-spirobi(indan)-4,4′,7,7′-tetrabromo-5,5′,6,6′-tetraol) and $[\{Co(Me_2tpa)\}_2(Br_2spiro)]^{2+}$ (**9**; Me_2tpa = bis(6-methyl-2-pyridylmethyl)(2-pyridylmethyl)amine), which are both in LS-Co^{III}-cat charge distributions at room temperature.[14] The shift of the LMCT energy from 14,837 cm^{-1} in **8** to 12,361 cm^{-1} in **9**, indicating a reduction in the energy gap between the LS-Co^{III}-cat ground state and HS-Co^{II}-sq excited state, foreshadows a lack of a VT transition in **8** but the observation of one in solid samples of **9**. The transition, however, is incomplete up to 360 K.

The first oxidation of precursor complexes $[Co(L_2^{R,R'})_2]^{2+}$ ($L_2^{R,R'}$ = *N*-(4-*R*-phenyl)-*N*-(4-*R′*-phenyl)-6-(1,10-phenanthrolin-2-yl)pyridine-2-amine) may be centered either on the cobalt center or on the triarylamine (Tara) unit, depending on the R group chosen, and hence, the oxidized complexes $[Co(L_2^{Me,Me})_2]^{3+}$ (**10**) and $[Co(L_2^{OMe,Me})_2]^{3+}$ (**11**) bear the potential to exhibit an equilibrium between Co^{III}-Tara and Co^{II}-$Tara^+$ redox isomers. In both of these cases, LMCT (Tara → Co^{III}) absorptions observed in the near-IR spectra in MeCN solution (the broad bands from 9,000 to 15,000 cm^{-1} in Fig. 6) are indicative of a Co^{III}-Tara redox isomer. Interestingly, Gaussian profile fitting reveals that the LMCT bands are split into two components, perhaps due to a Jahn-Teller distortion, or, alternatively, to a lifting of the doublet degeneracy of the $(t_{2g})^6(e_g)^1$ excited state by the asymmetry of the [Co^{II}(Tara)($Tara^+$)] redox isomer.

Replacing one of the methyl groups in **10** with a methoxy group to give **11** is expected to stabilize the Co^{II}-$Tara^+$ tautomer – the spectra in MeCN substantiate this prediction, with the energy of the lowest energy LMCT band lowering by 925 cm^{-1} from **10** to **11**. Accordingly, in **11**, the redox isomers are close enough in energy that the Co^{II}-$Tara^+$ state is marginally populated, as evidenced by the weak $Tara^+$ absorption (the sharper band at 12,100 cm^{-1} overlapping the LMCT band in Fig. 6), while in **10**, the energy separation between redox isomers is large enough that the Co^{II}-$Tara^+$ state is completely absent.

Furthermore, the solvent dependence of the LMCT bands can hint as to which solvents might stabilize one tautomer over the other. The red shift of the lowest energy LMCT band of **10** by 1,375 cm^{-1} upon changing the solvent from MeCN to DCM indicates that the Co^{II}-$Tara^+$ tautomer is relatively stabilized more so in DCM than in MeCN. Indeed, compared to the weak $Tara^+$ absorption exhibited by **11** in MeCN, the spectrum in DCM becomes dominated by a dramatically intensified $Tara^+$ absorption, indicating a significant shift to the Co^{II}-$Tara^+$ side of the equilibrium. Solvent dependence of the LMCT band energies of one complex can therefore be used to predict solvent induced changes in the VT equilibrium of another, in cases where the two complexes are closely related.

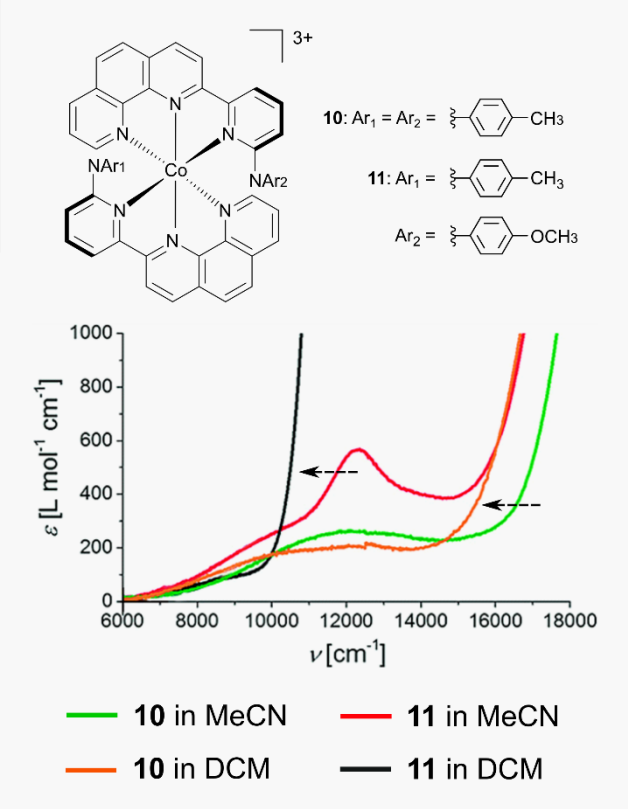

Fig. 6 Ligand tuning in **10** and **11**, with solvent-induced VT in the latter. Arrows illustrate the change in solvent from MeCN to DCM. Adapted with permission from Ref. [68]. Copyright © 2018 John Wiley and Sons.

The threshold for how low the energy of the charge transfer band must become to observe redox isomerism is specific to the particular system (Table 1). However, if one system is very similar to another, it may be possible to make useful comparisons between them. The complexes $[Co(L_3^{Me})_2]^{3+}$ (**12**) and $[Co(L_3^{OMe})_2]^{3+}$ (**13**; L_3^R = *N*,*N*-bis(4-*R*-phenyl)-4′-phenyl-[2,2′:6′,2″-terpyridine]-6-amine) are closely related to **10** and **11** – all bear triarylamine moieties attached to a meridional terdentate ligand, possess a Co^{III}-Tara ground state in MeCN, and exhibit two LMCT bands in the vis-NIR region.[69] The replacement of both methyl groups with methoxy groups in moving from **12** to **13** results in a red shift of the lower energy LMCT band of 1,350 cm^{-1}. Despite the shift, the lower energy LMCT band in **13** still lies slightly higher in energy than the equivalent band in **10** (11,751 cm^{-1} vs. 11,628 cm^{-1}), which does not display solvent induced redox isomerism. Hence, solvent induced redox isomerism is not to be expected in **13**. Indeed, while a DCM solution of **13** exhibits red shifted LMCT bands, the sharp absorption band that would mark the presence of the Co^{II}-$Tara^+$ tautomer remains absent.

An electronic structure analysis via DFT found low lying LMCT states, providing a good indication that thermally induced VT in related systems could be made possible by further reducing the energy of the open shell formulations. One disadvantage of the design of complexes **10** to **13** is that one of the aryl components of the triarylamine is involved in coordination to the metal center, resulting in an electron withdrawing effect from the amine nitrogen which destabilizes the Co^{II}-$Tara^{+}$ tautomer. By isolating the triarylamine moiety from the first coordination sphere, thermally induced VT was observed in the complex $[Co(L)_2]^{3+}$ (L = *ortho*-substituted 2-(pyridine-2-yl)-1,10-phenanthroline).[86] However, no LMCT bands were observed in the spectra, due to the increased distance between redox centers.

A final case study of using charge transfer spectra to illuminate aspects of a potential VT equilibrium is offered by a family of square pyramidal [Co(*R*-salen)(L)]$^{+}$ complexes (*R*-salen = *N*,*N'*-bis(3-*tert*-butyl-5-*R*-salicylidene)-1,2-cyclohexanediamine). As in previous examples, the one-electron oxidation of the square planar precursor complex [Co(*R*-salen)] has the potential to occur at two sites – in this case, either the cobalt center or the phenolate moiety. Therefore, the oxidized complexes, which are widely used catalysts for polymerization and other reactions,[87–89] can exist as one of two redox isomers. One aspect of their utility is their diamagnetism evident from ^{1}H NMR spectroscopy in dimethylsulfoxide (DMSO) solution, where the absence of paramagnetic broadening indicates a Co^{III}-phenolate charge distribution.[90] However, in most other environments, the complexes exhibit paramagnetic behavior, indicative of the presence of a Co^{II}-phenoxyl state.

The response of charge transfer bands to ligand tuning can indicate which of these redox isomers are present in a given solution. The broad charge transfer band exhibited by [Co(*t*-Bu-salen)$(OH_2)]^{+}$ (**14**) is dependent on the identity of the axial ligand (the aqua ligand can be replaced by a variety of monodentate Lewis bases), and so is not likely to arise from a LLCT or π-to-π* transition on the phenoxy ligand of a Co^{II}-phenoxyl species.[90] Accordingly, it must arise from either a MLCT of a Co^{II}-phenoxyl species or a LMCT of a Co^{III}-phenolate species. Since the band energy decreases from **14** to its methoxy-substituted equivalent [Co(MeO-salen)$(OH_2)]^{+}$ (**15**), in which the phenoxyl radical should be better stabilized, the band must arise from a LMCT excitation, therefore indicating the contribution of a Co^{III}-phenolate state to the room temperature identity of the complex.[70] In combination with other spectroscopic results that reveal a paramagnetic component to the identity, these interpretations point toward either an equilibrium (corresponding to valence tautomerism) or a resonance (corresponding to Class II-III or Class III mixed-valence behavior) between Co^{II}-phenoxyl and Co^{III}-phenolate formulations. The authors note that it is not clear which of the two is a more

accurate description – the reality may lie somewhere in between complete localization and complete delocalization.

The complexes $\{[(pzTp)Fe^{III}]_4(CN)_{12}[Co^{II}(Tp^{EtOH})]_4\}^{4+}$ (**16**; $pzTp^-$ = tetra(pyrazol-1-yl)borate, Tp^{EtOH} = 2,2,2-tris(pyrazol-1-yl)ethanol) and $\{[(Tp^*)(NC)Fe^{III}]_2(CN)_4[Co^{II}(t\text{-Bu-bipy})]_2\}^{2+}$ (**17**; Tp^{*-} = hydrotris(3,5-dimethylpyrazol-1-yl)borate, *t*-Bu-bipy = =4,4′-di-*tert*-butyl-2,2′-bipyridine) exhibit a temperature induced switchability between LS-Fe^{III}/HS-Co^{II} and LS-Fe^{II}/LS-Co^{III} states.[41,71] This is similar to a VT transition, however, VT typically refers to processes in which charge is transferred between a metal and a ligand, and the behavior of **16** and **17** is more precisely termed a charge-transfer-induced spin transition (CTIST). The effect was first reported in Co-Fe Prussian blue analogues,[40,91] but interest has grown in molecular analogues and their solution-state behavior.[46] Since CTIST in molecular systems has been extensively covered in a recent review,[92] we will only mention a few examples, focusing on the relationship between charge transfer spectra and redox isomeric behavior.

For Fe-Co CTIST systems, the relative intensities of the Fe^{II}-to-Co^{III} and Co^{II}-to-Fe^{III} charge transfer bands can qualitatively report on the position of the CTIST equilibrium. The solid-state thermochromism of **16**, characterized by a decrease in the Co^{II}-to-Fe^{III} band intensity and an increase in the Fe^{II}-to-Co^{III} band intensity with cooling, is a reflection of the change in ground state from LS-Fe^{III}/HS-Co^{II} at high temperatures (T > 248 K) to LS-Fe^{II}/LS-Co^{III} at low temperatures (T < 248 K).[41] The thermochromism of **17** was reported in solution (Fig. 7), and can be analyzed in much the same way as **16**, albeit with a lower switching temperature of 227 K and slightly shifted MMCT band energies.[71]

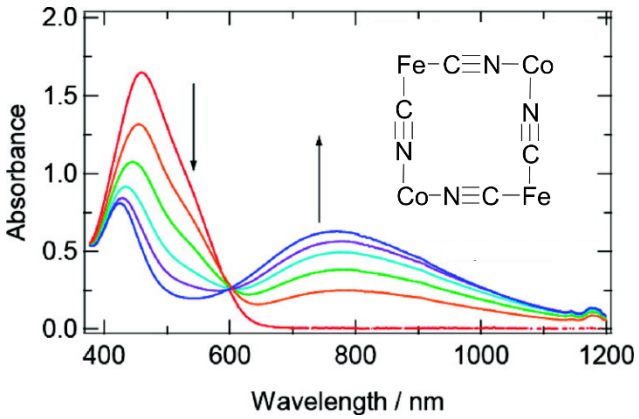

Fig. 7 The thermochromism of **17** in butyronitrile. Cooling from 300 K to 200 K is accompanied by the growth of a Fe^{II}-to-Co^{III} band at 770 nm and the decrease of the Co^{II}-to-Fe^{III} shoulder at 550 nm. Adapted from with permission from Ref. [71]. Copyright © 2011 American Chemical Society.

Similar to valence tautomerism, CTIST transitions can be optically induced. Above, we have discussed results indicating that the optically induced VT process proceeds via a two-step mechanism, whereby charge transfer to a LS-Co^{II} state precedes spin transition to a HS-Co^{II} state.[80] In contrast, a femtosecond resolved XANES study on a Co-Fe PBA demonstrated that in optically induced CTIST, the spin transition precedes the charge transfer.[39] After excitation of the LS-Co^{III}/LS-Fe^{II} species at 583 nm, the initially formed excited state, LS-Co(III)*/LS-Fe(II), decays in 50 fs to a HS-Co^{III}/LS-Fe^{II} state, whereupon charge transfer in 200 fs to the metastable HS-Co^{II}/LS-Fe^{III} state occurs. The study again demonstrates the utility of ultrafast XANES spectroscopy in elucidating the electronic dynamics of charge transfer phenomena.

Solvatochromism in non-redox-isomeric cobalt complexes

While thermochromism, as seen for **16** and **17**, involves temperature-induced spectral changes, solvatochromism, on the other hand, involves solvent-induced spectral changes. When these changes occur in the visible region, solvatochromism results in readily apparent color differences between solutions in different solvents. It is well known that a solution of cobalt(II) chloride is pink in water, bluish-violet in MeOH, and a striking deep blue in acetone and other organic solvents, which is due to solvent effects on an equilibrium between tetrahedral and octahedral species.[93] This is the simplest example in a wide range of solvatochromic cobalt compounds. Among these, there is a rich variability in the solvatochromic behavior, with solvent dependence having been observed for both tetrahedral and octahedral complexes, for both Co(II) and Co(III) complexes, and for transitions of a MLCT, LMCT, MMCT, and d-d nature. In this section, we survey the behavior of some pertinent examples, whose formulae are shown in Table 2, and structures in Fig. 8.

Table 2 Selected non-redox-isomeric cobalt complexes and the solvent parameters that are associated with their solvatochromic behavior. Structures are shown in Fig. 8.

Complex[a]	Number	Nature of solvatochromic band/s [b]	Relevant parameter[c]	Ref.
$[Co^{II}(2\text{-aminopyrimidine})_2(SCN)_2(OH_2)]$	**18**	d-d	DN	94
$[Co^{III}(acacen)(thioacetamide)_2]^+$	**19**	LLCT	DN	95
$[Co^{III}(salophen)(thioacetamide)_2]^+$	**20**	LLCT	DN	96
$[Co^{III}(bzacen)(thiobenzamide)_2]^+$	**21**	LLCT	DN	97
$[Co^{III}(saox)(bipy)_2]^+$	**22**	d-d	None	98
$[Co^{III}L_4^{N3O3}]$	**23**	d-d	AN	99
$[Co^{III}(L_5)_2]^-$	**24**	d-d	None	63
$[Co^{III}(5,5'\text{-dimethyl-2,2'-bipyridine})_2(ortho\text{-catecholate})]^+$	**25**	LMCT	$E_T(30)$	20

[a] Abbreviations (in order mentioned): **H_2saox** = salicylaldoxime, **$(L_4^{N3O3})^{3-}$** = 1,4,7-triazacyclononane-*N*,*N*′,*N*″-tripropionate, **H_2acacen** = bis(acetylacetone)ethylenediamine, **H_2salophen** = *N*,*N*′-bis(salicylidene)-1,2-phenylenediimine, **H_2bzacen** = bis(benzoylacetone)ethylenediamine, **H_2L_5** = 2-amino-1-(2-hydroxybenzamide)-2-methylpropane.

[b] Ligand-to-ligand charge transfer (LLCT).

[c] Donor number (DN), acceptor number (AN).

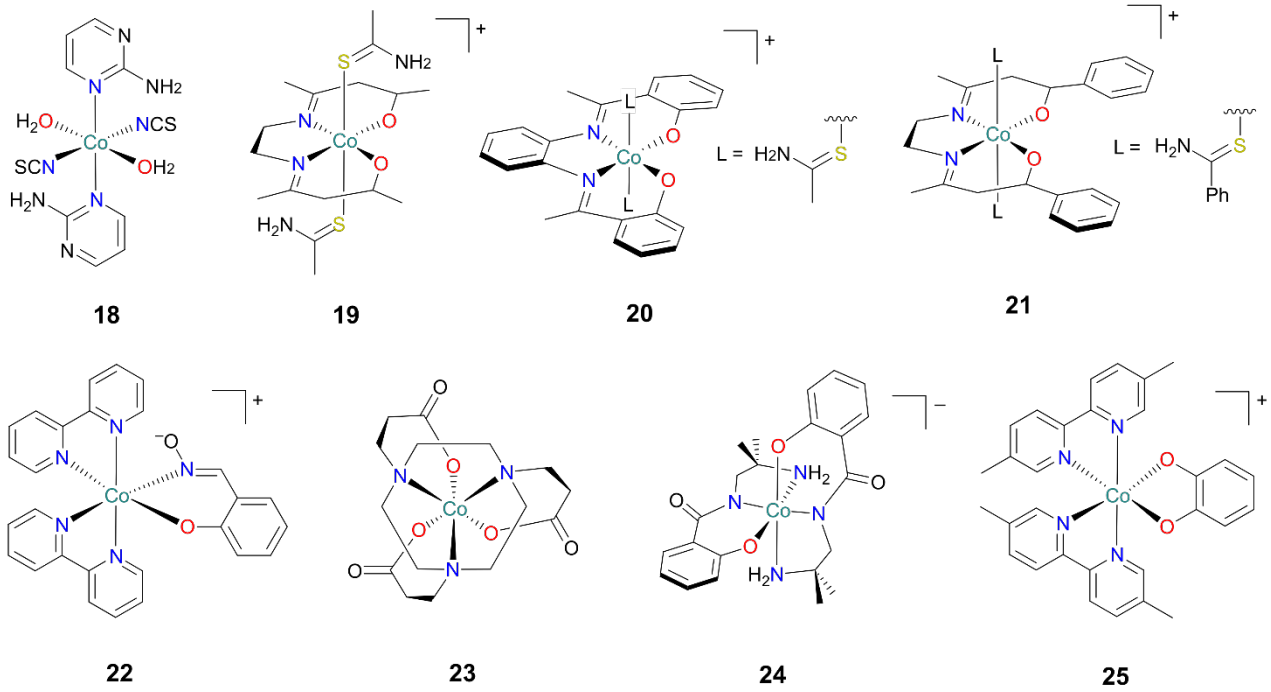

Fig. 8 Structures of complexes in Table 2.

In the case of d-d transitions, it is unlikely that the solvent dependence is due to dipole effects, since the permanent dipole should not change dramatically between ground and excited states. Rather, it most often arises from solvent effects on the crystal field splitting energy. In the simplest cases, this is caused by a change in species due to substitution of weakly coordinating ligands. Large changes in the shape and intensity of d-d bands typically characterize this behavior, as observed in $[Co^{II}(2\text{-aminopyrimidine})_2(SCN)_2(OH_2)]$ (**18**), in which d-d bands at 478 and 510 nm in methanol (MeOH) shift to 561 and 627 nm in MeCN, with the intensity of the lower energy band increasing about threefold and the shape becoming more asymmetric.[94] The authors describe replacement of the aqua ligands by MeCN, and it is unclear whether the effect is reversible.

Effects in the first coordination sphere also govern the solvatochromism of $[Co^{III}(acacen)(thioacetamide)_2]^+$ (**19**; H_2acacen = bis(acetylacetone)ethylenediamine), $[Co^{III}(salophen)(thioacetamide)_2]^+$ (**20**; H_2salophen = *N*,*N′*-bis(salicylidene)-1,2-phenylenediimine), and $[Co^{III}(bzacen)(thiobenzamide)_2]^+$ (**21**; H_2bzacen = bis(benzoylacetone)ethylenediamine). An absorption in the visible region (between around 450 to 600 nm, depending on the complex) shifts to shorter wavelengths as the solvent donor number is increased, due to a reversible equilibrium involving substitution of the axial ligands by coordinated solvent.[95–97]

For $[Co^{III}(saox)(bipy)_2]^+$ (**22**; H_2saox = salicylaldoxime), specific solvent-solute interactions cause changes in Δ_{oct} that in turn, affect the energies of the $^1A_{1g}\rightarrow{}^3T_{1g}$ and $^1A_{1g}\rightarrow{}^3T_{2g}$ transitions.[98] In this case, the band wavelengths do not correlate with any of the solvatochromic parameters discussed earlier. When a correlation can be made, it is possible to draw insights into the solvent-solute interactions, for example, in the case of $[Co^{III}L_4^{N3O3}]$ (**23**; $(L_4^{N_3O_3})^{3-}$ = 1,4,7-triazacyclononane-*N*,*N′*,*N″*-tripropionate), in which the dependency of ν_{max} on the solvent acceptor number was attributed to effects in the second coordination sphere.[99] Interactions between acceptor solvent molecules and lone pairs on the carboxylate oxygen atoms weaken both σ and π bonding between metal and ligand. In this case, the π interaction is dominant. Weakened π bonds result in larger values of Δ_{oct}, causing a blue-shift of the d-d transitions with increasing acceptor strength.

A curious example of d-d bands varying in intensity but not in wavelength occurs in $[Co^{III}(L_5)_2]^-$ (**24**; H_2L_5 = 2-amino-1-(2-hydroxybenzamide)-2-methylpropane). A change in species, as in **18**, is ruled out via ^{1}H NMR spectroscopy – rather, it is proposed that the wide

color variability (Figure 9) is due to breaking molecular symmetry by specific solvent-solute interactions, which alters the oscillator strength of the transitions.[63] This theory is supported by a further study on two different salts of **24**. Although the crystals visually differ in color, diffuse reflectance spectra revealed no differences in the band wavelengths – therefore, the observed color change must be due to changes in band intensities.[100] Between the crystal structures of the two salts, the Co-N/O bond lengths did not differ – however, the molecular symmetry was lowered from one salt to another, potentially resulting in changes in transition oscillator strengths.

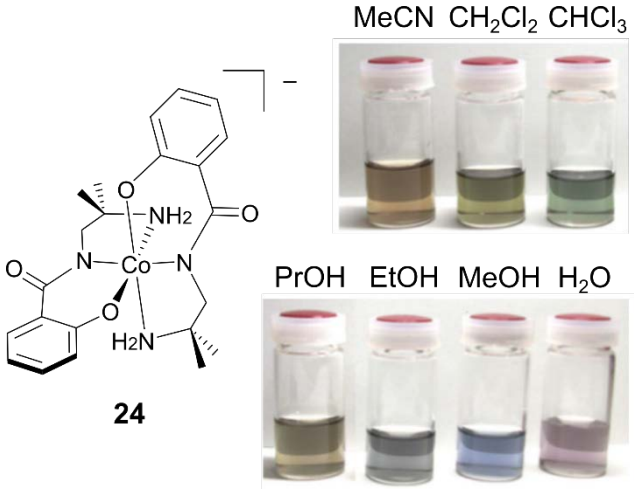

Fig. 9 The diverse range of colors exhibited by various solutions of (PPh_4)**24** (1.0 x 10^{-3} M). Reprinted from Ref. [63], Copyright © 2013, with permission from Elsevier.

Moving to solvatochromism relating to charge transfer bands, an experimental and computational study of [Co^{III}(5,5′-dimethyl-2,2′-bipyridine)$_2$(*ortho*-catecholate)]$^+$ (**25**) is illustrative in demonstrating the information that can be gained from analysis of solvatochromic behavior. The compound's negative solvatochromism is consistent with calculated values of the ground and excited state dipole moments of 13.33 D and 9.26 D, respectively.[20] Natural transition orbital analysis revealed that the solvent dependent excitation is a d-d ($d_{yz} \longrightarrow d_{z2}$) transition with significant LMCT character due to significant contributions to the donor state from a filled π* orbital on the catecholate ligand. Thus, the excited state can be interpreted as having some aspects of a transient Co^{II}-sq valence tautomer.

A linear correlation was found between λ_{max} values of **25** in various solvents and the Reichardt E_T(30) parameter. However, estimates of the excitation energy calculated by time

dependent DFT (TD-DFT) did not correlate with the experimentally observed excitation energies, with non-hydrogen bonding solvents appearing to adhere to a linear trend from which hydrogen bonding solvents greatly deviated. The issue was that the calculations only captured the solvent's dielectric characteristics and were unable to account for specific solvent-solute interactions. When instead, the excitation energy model was amended to incorporate both ε_r as well as the Kamlet-Taft α-parameter, the agreement between calculated and experimental trends was greatly improved. Since the catecholate oxygen atoms are the most likely sites on the complex to accept hydrogen bonds, the authors explored the effect of replacing them with sulfur atoms, which should be weaker hydrogen bond acceptors. In the sulfur analogue, the experimentally observed solvatochromism was well reproduced by TD-DFT calculations, with inclusion of hydrogen bonding considerations not necessary. Conversely, when λ_{max} was plotted against $E_T(30)$, hydrogen bonding solvents did not conform to the linear trend obeyed by non-hydrogen bonding solvents. These findings are consistent with hydrogen bonding between catecholate oxygen atoms and solvent playing a significant role in the solvatochromism of **25**.

From this example, it can be seen that a simple plot of λ_{max} against $E_T(30)$ can give an indication of the hydrogen bonding interactions occurring in solution. In the case of negative solvatochromism, a linear correlation for all solvents would indicate that hydrogen bonding plays a significant role in stabilizing the ground state. This could have important ramifications for the solution-state behavior of valence tautomeric systems, in which the equilibrium is usually manipulated by redox tuning,[37] but sometimes also by solvent choice.[23,101] Hydrogen bonding interactions could conceivably stabilize one redox tautomer more than the other, allowing manipulation of the equilibrium via choice of solvent.

Solvatochromism and redox isomerism: valence tautomerism

In the following section, we discuss more general examples of solvent dependent VT equilibria, applying solvatochromic theory where possible to guide interpretations of this phenomenon. The stark color changes that often accompany the manipulation of a VT equilibrium via solvent choice arise less from the shifting of band energies, as seen for **23** and **25**, and more from the growth of bands associated with one tautomer and the bleaching of bands associated with the other tautomer. This is similar to the thermochromic behavior of **16** and **17**, except that in the following examples, spectral changes are induced by solvent, rather than temperature.

It is necessary, however, to introduce a parameter associated with thermally induced VT. The critical temperature, T_c, is the temperature at which the populations of both tautomers are equal – in other words, when ΔG_0 is zero.[3,12] For example, in Co-dioxolene systems, if T_c is above room temperature, then the LS-Co^{III}-cat tautomer is favored at room temperature, while if T_c is below room temperature, then the HS-Co^{II}-sq tautomer is favored. In the case of $[Co(Me_3tpa)(Br_4diox)]^+$ (**26,** see Table 3) previously described, the stabilization of the HS-Co^{II}-sq tautomer in chlorinated solvents can therefore be alternatively described as a decrease in T_c upon changing the solvent from MeCN to DCM.[23] The underlying spectral changes for **26** are depicted in Fig. 11 (top). In MeCN, acetone, and *N,N*-dimethylformamide (DMF), the LMCT bands centered around 414 and 803 nm are characteristic of a LS-Co^{III}-cat tautomer, while the spectra in chlorinated solvents DCE and DCM are dominated by MLCT bands in the 500-650 nm range and semiquinonate-based transitions at 432 nm and 700-1000 nm, suggesting that the HS-Co^{II}-sq tautomer dominates.[23] The higher value of T_c in MeCN compared to DCE and DCM can be monitored by variable temperature UV-vis spectroscopy. Heating MeCN solutions of **26** from 283 to 348 K results in a grow-in of the MLCT and semiquinonate features that dominate the DCE and DCM spectra (Fig. 11 (bottom)).

Table 3 Examples of solvatochromic complexes with two possible redox isomers, where some examples exhibit a redox isomeric equilibrium, and some do not. The solvent-dependent parameter is listed, as well as the solvatochromic parameter that correlates with it. Structures of the non-dioxolene complexes are shown in Fig. 10.

Complex[a]	Number	Redox isomerism?	Solvent-dependent parameter	Correlated solvatochromic parameter/s	Ref.
$[Co(Me_3tpa)(Br_4diox)]^+$	**26**	Yes	T_c	None	23
$[Co(Me_3tpa)(Cl_4diox)]^+$	**27**	Yes	T_c	DN	22
$[Co(L^{N4})(t\text{-}Bu_2diox)]^+$	**28**	Yes	T_c	None	101
$[Co^{II}(tmeda)(t\text{-}Bu_2diox)_2]$	**29**	Yes	T_c	DN	102
$[Co(py_2O)(3,6\text{-}t\text{-}Bu_2diox)_2]$	**30**	Yes	T_c	DN, ε_r	103
$[Mn(cth)(t\text{-}Bu_2diox)]^+$	**31**	Yes	T_c	DN, ε_r	104
$[Mn(pyridine)_2(t\text{-}Bu_2diox)_2]$	**32**	Yes	T_c	DN, ε_r	
$[Ru(NH_3)_4(t\text{-}Bu_2diox)]^{2+}$	**33**	Yes	ν(MLCT), ν(LMCT)	DN	105
$[Fe^{III}(cth)(t\text{-}Bu_2cat)]^+$	**34**	No	ν(LMCT)	DN, ε_r	106
$[Fe^{III}(tmeda)(t\text{-}Bu_2cat)_2]$	**35**	No	ν(LMCT)	DN	107
$[Co(Ph_2bipy)(t\text{-}Bu_2diox)_2]$	**36**	Yes	T_c	ε_r	38
$[(CuCl_2)_2(L_6)]$	**37**	Yes	T_c	ε_r	108
$[CuX_2(L_7)]$ (X = Cl, Br)	**38**	Yes	T_c	ε_r	109
$[Co_2(hmteta)(3,6\text{-}t\text{-}Bu_2diox)_4]$	**39**	Yes	T_c	DN, ε_r	110
$[M(Bu\text{-}py)_2(t\text{-}Bu\text{-}diox)_2]$, M = Mn, Co	**40^M**	Yes	T_c	DN, ε_r	111
$[Co(BzOEt\text{-}phen)(t\text{-}Bu\text{-}diox)_2]$	**41**	Yes	T_c	ε_r	112
$[Co(L_8)_2]$	**42**	Yes	T_c	None	113
$[Fe^{III}(bispicen)(Cl_4diox)_2]$	**43**	No	ν(LMCT)	None	114
$[Co(L^{N2})(t\text{-}Bu_2diox)_2]$	**44**	Yes	T_c	None	115
[Fc-NHCO-Cc]$^+$	**45**	No	ν(MMCT)	Correlates with a function of the Kamlet-Taft parameters[25]	116
[Fc-NHCO-Cc-CONH-Fc]$^+$	**46**	No	ν(MMCT)	See **45**	116
$[\{L^{N5}Co^{III}(\mu\text{-}NC)\}_2Fe^{II}(CN)_4]^{2+}$	**47**	No	ν(MMCT)	ε_r	18

[a] Abbreviations (in order mentioned): **Br_4diox** = tetrabromodioxolene, **Cl_4diox** = tetrachlorodioxolene, **L^{N4}** = *N*,*N*′-diisopropyl-2,11-diaza[3.3]-(2,6)pyridinophane, **tmeda** = *N,N,N′,N′*-tetramethylethylenediamine, **py_2O** = dipyridyl ether, **3,6-*t*-Bu_2diox** = 3,6-di-*tert*-butyldioxolene, **Ph_2bipy** = 4,4′-diphenyl-2,2′-bipyridine, **L_6** = 2,3,5,6-tetrakis(tetramethylguanidino)pyridine, **L_7** = 5,6-bis-(*N,N′*-dimethyl-*N,N′*-ethylene-guanidino)-2,2-dimethyl-[1,3]-benzodioxole, **hmteta** = 1,1,4,7,10,10-

hexamethyltriethylenetetramine, **Bu-py** = 4-*tert*-butylpyridine, **BzOEt-phen** = ethyl 4-(1,10-phenanthrolin-5-yl)benzoate, **HL_8** = 3,5-di-*tert*-butyl-1,2-quinone-1-(2-hydroxy-3,5-di-*tert*-butylphenyl)imine, **bispicen** = *N,N′*-bis(2-pyridylmethyl)-1,2-ethanediamine, **L^{N_2}** = 2,2′-bipy or 1,10-phenanthroline, **Cc** = cobaltocenyl, **L^{N_5}** = 6-methyl-1,4,8,11-tetraaza-cyclotetradecan-6-amine.

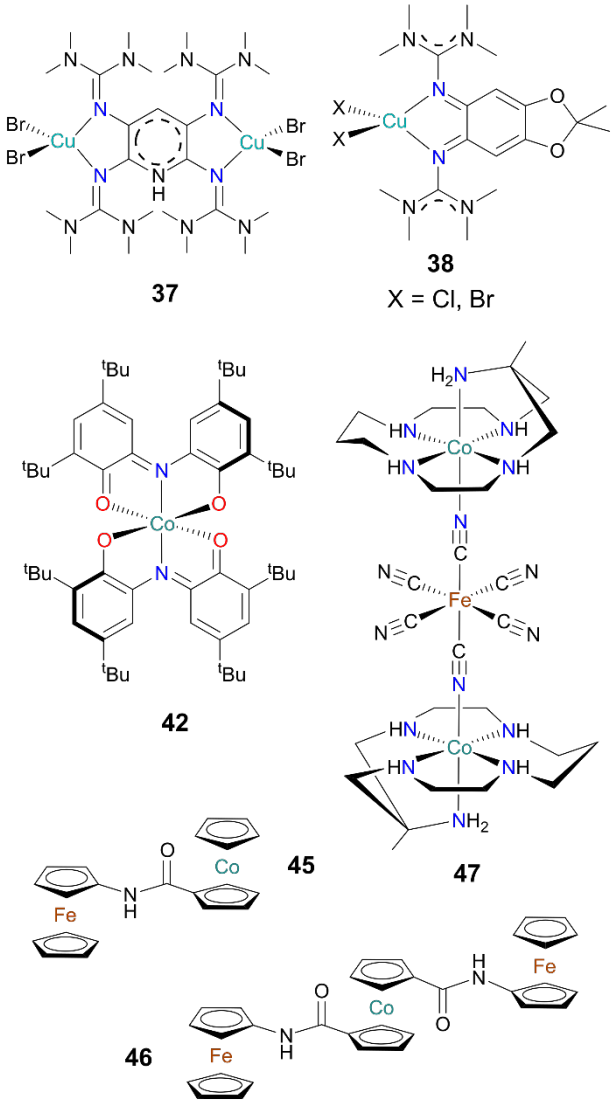

Fig. 10 Structures of the non-dioxolene complexes in Table 3.

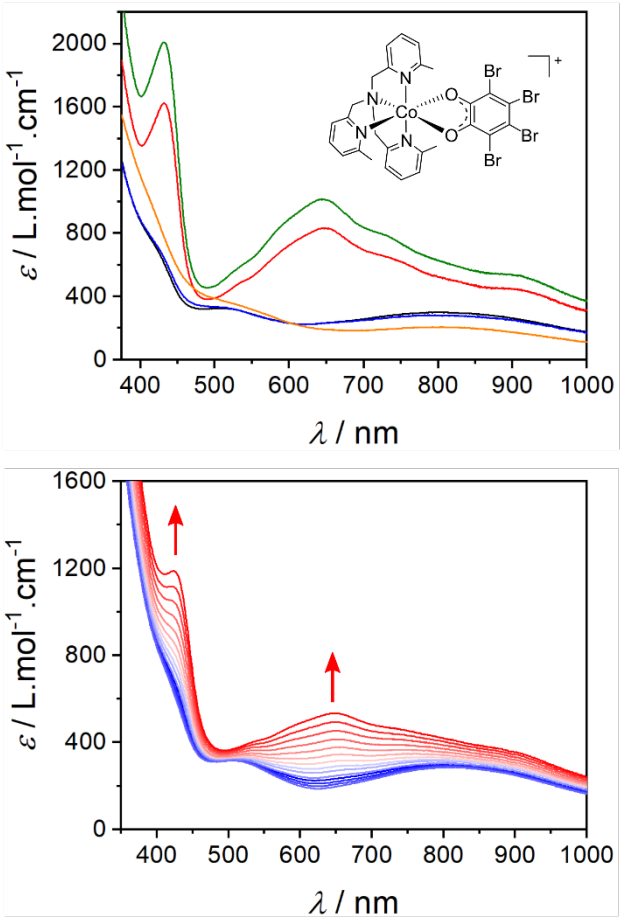

Fig. 11 Top: UV-vis spectra of **26** in MeCN (black), acetone (blue), DMF (orange), DCE (red), and DCM (green), illustrating its solvatochromic behavior. The broken line on the catechol ligand indicates its oxidation state of either –1 or –2, depending on the temperature and solvent. Bottom: Variable temperature UV-vis spectra of **26** in MeCN from 283 K (blue) to 348 K (red) in 5 K intervals.[23]

The stabilization of the HS-Co^{II}-sq tautomer in halogenated solvents has also been observed for the complexes [Co(Me$_3$tpa)(Cl$_4$diox)]$^+$ (**27**; Cl$_4$diox = tetrachlorodioxolene) and [Co(L^{N_4})(*t*-Bu$_2$diox)]$^+$ (**28**; L^{N_4} = *N*,*N*′-diisopropyl-2,11-diaza[3.3]-(2,6)pyridinophane),[22,101] and we have already discussed that DCM stabilizes the Co^{II}-Tara$^+$ tautomers of complexes **10** and **11**. In a study of **27** it was argued that solvents of high donor number (MeCN, DMSO, and acetone), and therefore high Lewis basicity, favor the LS-Co^{III}-cat tautomer, while the chlorinated solvents DCM and DCE favor the HS-Co^{II}-sq tautomer.[22] Similarly, solution state magnetic susceptibility measurements (Evans NMR method) on **28** revealed that T_c is lower in DCE and 1,2-dibromoethane (DBE) than in MeCN, with the halogenated solvents again favoring the HS-Co^{II}-sq tautomer (Fig. 12).[101]

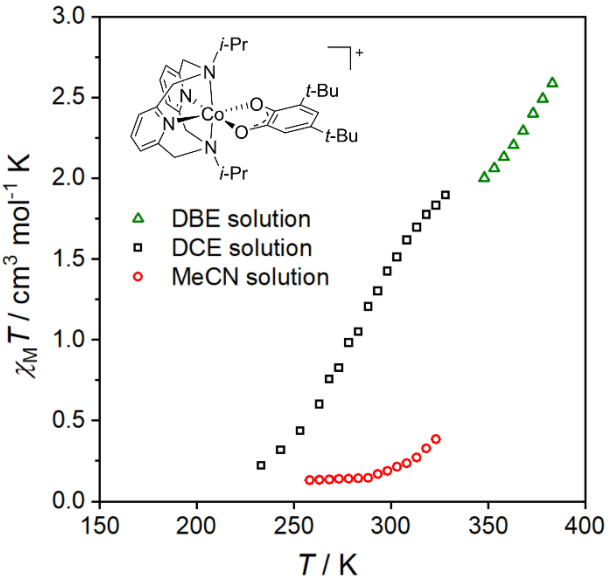

Fig. 12 Solution state magnetic susceptibility measurements on **28** by the Evans NMR method in DCE-d_4 (black squares), DBE-d_4 (green triangles), and MeCN-d_3 (red circles).[101] In all solvents, incomplete transitions occur over the temperature ranges measured, which depend on the liquid range of the solvent and the solubility of the compound. With increasing temperature, $\chi_M T$ increases, consistent with a transition between diamagnetic Co^{III}-cat and paramagnetic Co^{II}-sq.

Various solvatochromic parameters have been used in to characterize solvent dependency of VT equilibria. The solvatochromic behaviors of the complexes discussed in this section and the next are summarized in Table 3. There are numerous examples in support of a donor number argument such as that put forward for **27**, whereby an increase in the solvent donor number results in an increased stabilization of the state with a smaller metal center. In $[Co^{II}(tmeda)(t\text{-}Bu_2diox)_2]$ (**29**; tmeda = *N,N,N′,N′*-tetramethylethylenediamine), the increase in T_c in the order toluene < DCM < MeCN < DMF matches the trend in donor number.[102] The same trend between T_c and solvent donor number is observed in $[Co(py_2O)(3,6\text{-}t\text{-}Bu_2diox)_2]$ (**30**; py_2O = dipyridyl ether, 3,6-*t*-Bu_2diox = 3,6-di-*tert*-butyldioxolene).[103] The manganese complex $[Mn(cth)(t\text{-}Bu_2diox)]^+$ (**31**) is present as the blue-green Mn^{II}-sq tautomer in toluene and acetone, but changing the solvent to DMSO, with a comparatively higher donor number, results in a change in the solution color to yellow and an increase in the population of the Mn^{III}-cat state, evidenced in the UV-vis spectra.[104] Likewise, for the complex $[Mn(pyridine)_2(t\text{-}Bu_2diox)_2]$ (**32**), the VT equilibrium shifts from the Mn^{II}-$(sq)_2$ side to the Mn^{IV}-$(cat)_2$ side as the donor number increases with a change in solvent from toluene to pyridine.[117]

The solvatochromism of charge transfer bands observed for $[Ru(NH_3)_4(t\text{-}Bu_2diox)]^{2+}$ (**33**), $[Fe^{III}(cth)(t\text{-}Bu_2cat)]^{+}$ (**34**), and $[Fe^{III}(tmeda)(t\text{-}Bu_2cat)_2]$ (**35**) is consistent with the increasing stabilization of higher-valent metal forms with increasing solvent donor number.[105–107] For complexes **34** and **35**, no VT equilibrium is observed, however for both complexes, the negative solvatochromism of the LMCT band, defined by an increase in the band energy with increasing donor number, indicates that the Fe^{III}-cat ground state is increasingly stabilized relative to the Fe^{II}-sq excited state as the donor number increases.[106,107] Both Ru^{III}-sq and Ru^{II}-bq (benzoquinone) tautomers are present in solutions of **33**.[105] As the donor number increases, the LMCT band associated with a Ru^{III}-sq ground state increases in energy, while the MLCT band associated with a Ru^{II}-bq ground state decreases in energy (Fig. 13). Both observations are consistent with a stabilization of the Ru^{III}-sq tautomer relative to the Ru^{II}-bq tautomer as the solvent donor number increases.

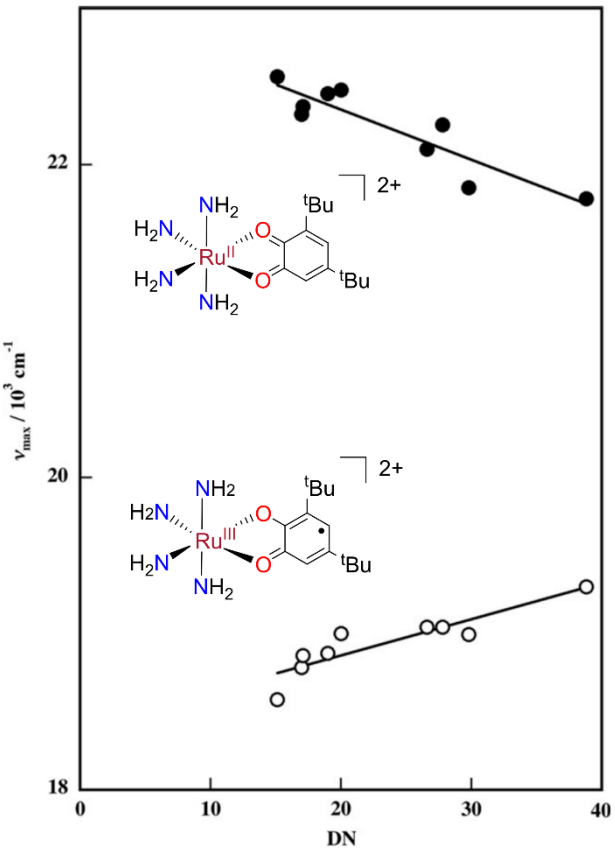

Fig. 13 Dependencies of the MLCT (●) and LMCT (○) band energies of **33** on the solvent donor number. The MLCT band arises from the Ru^{II}-bq tautomer, and the LMCT band from the Ru^{III}-sq tautomer, as shown. Reprinted from Ref. [105], Copyright © 2012, with permission from Elsevier.

Although the complex $[Fe^{II}(bzimpy)_2]^{2+}$ (bzimpy = 2,6-bis-(benzimidazol-2′-yl)-pyridine) displays not VT, but SCO, the increasing stabilization of the LS-Fe state with increasing donor number is consistent with the observation in the above examples that the state with a smaller metal center is increasingly favored as the donor number increases.[57]

In various other cases, it is changes in solvent polarity, rather than donor number, which is proposed to cause solvent dependence of VT equilibria. Solution-state UV-vis data of $[Co(Ph_2bipy)(t\text{-}Bu_2diox)_2]$ (**36**; Ph_2bipy = 4,4′-diphenyl-2,2′-bipyridine) suggest that T_c decreases as the polarity of the solvent, as indicated by the ε_r parameter, increases.[38] An alternative description of this behavior is that the HS-Co^{II}-sq tautomer is increasingly favored as ε_r increases. Although this is the opposite to what would be expected based on the seemingly larger charge separation in the LS-Co^{III}-cat tautomer, many examples of solvatochromic MLCT bands have shown that the connection between nominal charge distribution and dipole moment is not always obvious.[59,60] In one such example, a ruthenium complex with a Ru^{II}-L ground state and a Ru^{III}-$L^{\bullet-}$ excited state (L = 4,4′-COOH-2,2′-bipyridine) experiences a reduction in dipole moment upon excitation, contrary to what would be expected if considering the formulae alone.[59]

Solvent effects on VT equilibria have been observed for several copper complexes.[108,109,118] For dinuclear $[(CuCl_2)_2(L_6)]$ (**37**; L_6 = 2,3,5,6-tetrakis(tetramethylguanidino)pyridine), the Cu^{I}–L^{2+}–Cu^{I} tautomer is increasingly favored over the Cu^{II}-L-Cu^{II} tautomer as the solvent polarity increases.[108] This was shown by monitoring spectral changes arising from increasing the solvent polarity, first by adding successive increments of the salt $(NBu_4)PF_6$ to DCM solutions of the complex, then by the usual method of substituting DCM with a solvent with a higher ε_r value. Noteworthy here is the effect of electrolyte concentration on the VT equilibrium – this could potentially be important when preparing solutions for electrochemical measurements, which necessarily always contain a supporting electrolyte. As in **25**, the DFT-calculated dipole moments of the two possible electronic structures of **37** are consistent with the observed solvatochromic behavior; the Cu^{I}–L^{2+}–Cu^{I} tautomer exhibits a larger dipole moment, and therefore is favored by more polar solvents.

Similarly to **37**, in the mononuclear complexes $[CuX_2(L_7)]$ (**38**; X = Cl, Br; L_7 = 5,6-bis-(*N,N′*-dimethyl-*N,N′*-ethylene-guanidino)-2,2-dimethyl-[1,3]-benzodioxole) the population of the high temperature tautomer (Cu^{I}–L^{+} in this case) increases with the ε_r value of the solvent.[109] Here, double integration of the EPR signals was used to determine the relative populations of the Cu^{I}–L^{+} and Cu^{II}-L states.

While in **36** to **38**, it is the high temperature tautomer which is favored by more polar solvents, in reports of the complexes [Co_2(hmteta)(3,6-*t*-Bu_2diox)$_4$] (**39**; hmteta = 1,1,4,7,10,10-hexamethyltriethylenetetramine) and [M(Bu-py)$_2$(*t*-Bu-diox)$_2$] (**40^{M}**; M = Co, Mn; Bu-py = 4-*tert*-butylpyridine) it is suggested by their respective authors that the low temperature tautomers are favored by more polar solvents, or equivalently, that the high temperature tautomers are favored by more non-polar solvents.[110,111] For **39**, moving from THF or acetone to non-polar toluene shifts the equilibrium toward the Co^{II}-sq tautomer.[110] Pyridine solutions of **40^{Co}** favor a Co^{III}-cat electronic structure, but as the non-polar toluene component of mixed pyridine/toluene solutions is increased, the Co^{II}-sq tautomer is increasingly favoured.[111] The same behavior is observed in **40^{Mn}**, albeit between Mn^{IV}-cat and Mn^{III}-sq charge distributions.[111] Similarly, in the complex [Co(BzOEt-phen)(*t*-Bu-diox)$_2$] (**41**; BzOEt-phen = ethyl 4-(1-10-phenanthrolin-5-yl)benzoate), T_c shifts from 261-265 K to 230-231 K upon moving from DCM to toluene.[112]

It is important to note that for several of these examples, solution-state equilibria were investigated in only two or three solvents. More detailed solvatochromic analyses can often be precluded by insolubility or dissociation/decomposition in certain solvents.[23,111] Solvatochromic effects between pyridine and toluene in **40^{Co}** and **40^{Mn}** could be due to polarity, but equally, they could be due to donor number, with pyridine of stronger donicity favoring the Co^{III}-cat and Mn^{IV}-cat forms.

In many cases, therefore, it can be difficult to determine the specific environmental interactions responsible for solvent effects on VT equilibria. In one such case, the T_c of the complex [Co(L_8)$_2$] (**42**; HL_8 = 3,5-di-*tert*-butyl-1,2-quinone-1-(2-hydroxy-3,5-di-*tert*-butylphenyl)imine) falls by around 60 K when the solvent is changed from toluene to the commercially available oil Miglyol 812 – but due to the uniqueness and relative lack of solvatochromic data for the latter solvent, it is difficult to make any conclusions about the environmental interactions.[113] The solvent-solute interactions can also remain ambiguous when solvatochromic trends do not correlate with any solvatochromic parameters – for example, the T_c trend exhibited by **26** fails to correlate with donor number or ε_r, or indeed, any of the solvatochromic parameters mentioned in the theory section of this review. Similarly, for the complex [Fe^{III}(bispicen)(Cl_4diox)$_2$] (**43**; bispicen = *N,N′*-bis(2-pyridylmethyl)-1,2-ethanediamine), the separation between Fe^{III}-cat ground and Fe^{II}-sq excited states, as measured by the LMCT energy, increases in the order MeOH < DMF < MeCN, a trend that agrees neither with donor number or polarity.[114]

Addressing the lack of a correlation between T_c and ε_r in the complexes [Co(L^{N_2})(*t*-Bu_2diox)$_2$] (**44**; L^{N_2} = 2,2′-bipy, 1,10-phenanthroline), it was noted, in a detailed study on solution VT, that the endoergic term (Ω) may play an important role.[115] Also known as the cavity term, Ω measures the work involved in separating solvent molecules to create a cavity accommodating the solute molecule.[27,119] As cobalt VT systems are associated with a particularly large bond length changes, due to the low-spin-to-high-spin transition that accompanies charge transfer, Ω may be especially relevant to them. During the LS-Co(III)-to-HS-Co(II) transition, the molecular expansion necessitates an expansion of the solvent cavity. The work associated with this will increase as the Ω value of the solvent increases – hence, solvents with a larger Ω value could conceivably stabilize the LS-Co(III) isomer relative to solvents with a smaller Ω value. To the best of our knowledge, the effects of Ω on VT equilibria have not been mentioned elsewhere. However, it would be an interesting factor to consider, particularly in cobalt VT systems in which T_c does not correlate with the usual solvatochromic parameters.

Taken altogether, the solvatochromic behavior of the complexes discussed in this section suggest that, although solvent trends in T_c, ν(LMCT), or ν(MLCT) can usually be explained on the basis of solvent donor number or polarity, the several systems that do not obey either of these trends illustrate the potential importance of specific solvent-solute interactions. For example, halogen interactions in **26** could play a role in the stabilization of the Co^{II}-sq tautomer in chlorinated solvents. The effect of Ω, moreover, would be dependent on the molecular volume change associated with the transition, a specific value that would vary between systems.[119]

Solvatochromism and redox isomerism: charge-transfer-induced spin transition

For systems where the charge transfer excited state is an electrochemically accessible species, the energy of the charge transfer absorption (E_{op}) can be related to the free energy difference (ΔG_0) between two redox isomers. For solvatochromic compounds, E_{op} is solvent dependent. However, solvent-induced changes in E_{op} cannot necessarily be used to infer changes in ΔG_0, as the following shall illustrate.

The MMCT bands of the heterometallocenes [Fc-NHCO-Cc]$^+$ (**45**; Cc = cobaltocenyl) and [Fc-NHCO-Cc-CONH-Fc]$^+$ (**46**) both exhibit negative solvatochromism.[116] With closed

shell Fe^{II}-Co^{III} ground states, the Fe^{III}-Co^{II} excited states represent potential CTIST redox isomers. Since E_{op} in **45** falls by around 2,500 cm^{-1} from MeCN to DCM, it would be tempting to infer that DCM stabilizes the Fe^{III}-Co^{II} redox isomer. However, the value of ΔG_0 (estimated via electrochemical measurements) changes minimally between the two solvents. The same behavior is observed across a range of Fe-Co heterometallocenes (strong solvent dependency of E_{op} but comparatively weak solvent dependency of ΔG_0), indicating that in these systems the solvatochromism arises principally from changes in λ rather than changes in ΔG_0 [see eqn (1)].[17]

Compared to Fe-Fe bimetallocenes, the Fe-Co heterometallocenes **45**, **46**, and the prototype molecule they are based on, $[Fc\text{-}Cc]^+$, exhibit enhanced metal-to-metal communication.[120] To investigate their potential as switchable molecules, energy diagrams for **45**, **46**, and $[Fc\text{-}Cc]^+$ were constructed based on a two state Hush model (Fig. 14).[116] As ΔG_0 lowers from 1.58 V in $[Fc\text{-}Cc]^+$ to 1.135 V in **45** and 0.95 V in **46**, the system approaches a double well potential. For genuine redox isomerism in Fe-Co heterobimetallocenes, ΔG_0 must be lowered even further.

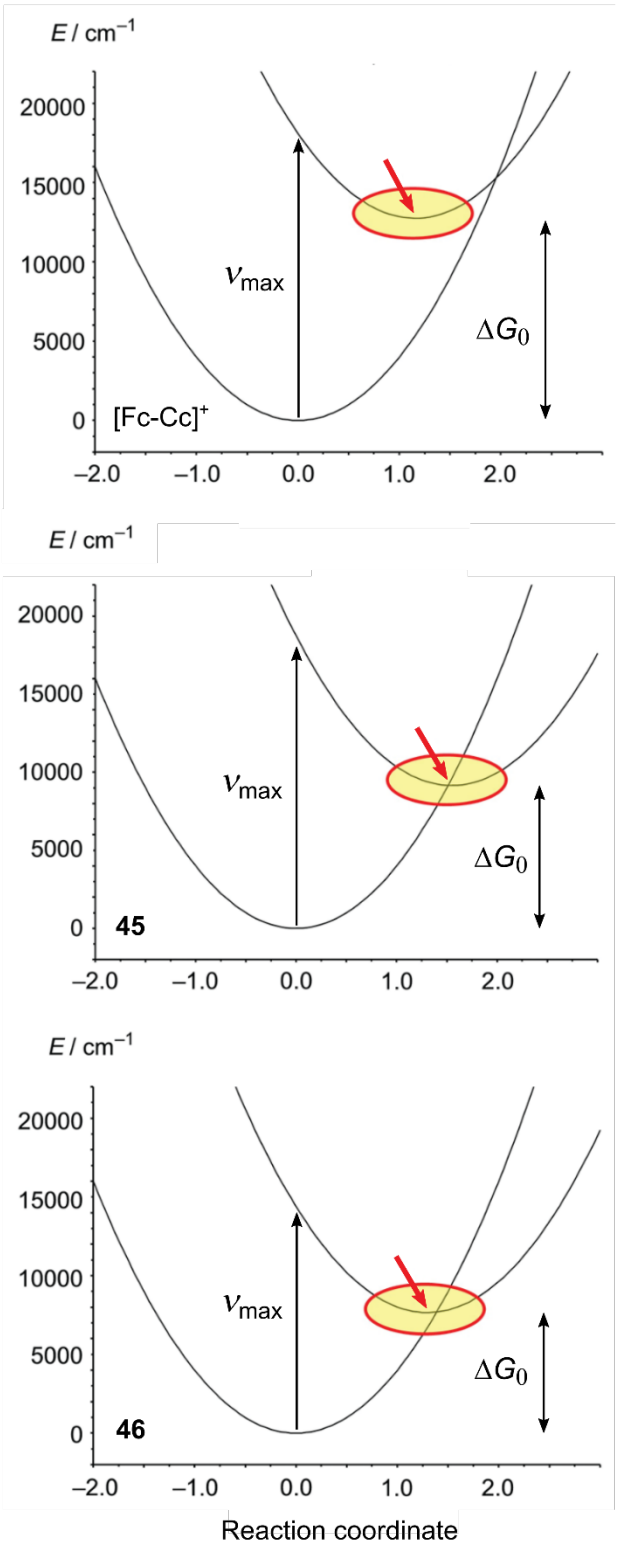

Fig. 14 Hush diagrams for $[Fc\text{-}Cc]^+$ (top), **45** (middle), and **46** (bottom), constructed based on MMCT energies determined spectroscopically and ΔG_0 values estimated via electrochemical measurements. The excited state minima are highlighted and indicated by red arrows. Adapted with permission from Ref. [116]. Copyright © 2012 American Chemical Society.

A study on a series of cyano-bridged Fe^{II}-Co^{III} systems found that, as in Fe-Co heterometallocenes, the solvatochromic behaviors of the MMCT bands were primarily due to changes in λ rather than changes in ΔG_0, as in **45** and **46**.[121] However, the effects of ligand tuning on E_{op} resulted primarily from changes in ΔG_0, with λ only varying marginally. Hence, changes in E_{op} caused by ligand tuning can be used to infer changes in the relative stabilization of the redox isomeric Fe^{III}-Co^{II} MMCT excited state. For instance, in the dinuclear species $[(L)Co(NC)Fe(CN)_5]^{2-}$ (L = 6-methyl-1,4,8,11-tetraazacyclotetradecan-6-amine), replacement of two of the cobalt-bound NH groups with sulfur atoms causes the MMCT to drop by 2,100 cm^{-1}, corresponding to a stabilization of the Fe^{III}-Co^{II} state.[122] Likewise, the MMCT energy of the very similar complex $[(L)Co(NC)Fe(CN)_5]^{2-}$ (L = 10-methyl-1,4,8,12-tetraazacyclopentadecan-10-amine) increases with decreasing pH, corresponding to a stabilization of the Fe^{II}-Co^{III} state due to protonation of the iron-bound cyanide ligands.[123]

For the closely related trinuclear complex $[\{L^{N_5}Co^{III}(\mu\text{-}NC)\}_2Fe^{II}(CN)_4]^{2+}$ (**47**; L^{N_5} = 6-methyl-1,4,8,11-tetraaza-cyclotetradecan-6-amine) the MMCT band exhibits a negative solvatochromism.[18] Notably, the solvatochromism is not limited to changes in E_{op} – in addition, the intensity of the MMCT band increases dramatically with an increase in the solvent donor number. Since, according to the Hush model, ε_{max} is related to the electronic coupling, H_{ab}, between donor Fe^{II} and acceptor Co^{III} units by

$$H_{ab} \propto \frac{\sqrt{\varepsilon_{max}\lambda_{max}\Delta\nu_{1/2}}}{r_{DA}}, \quad (2)$$

where $\Delta\nu_{1/2}$ is the MMCT bandwidth at half-height and r_{DA} is the distance between donor and acceptor units,[43,124,125] trends in ε_{max} could potentially be qualitatively reporting on trends in H_{ab}, and therefore on solvent-induced changes in the extent of charge delocalization between the two metals. In this case, the compound exhibits a localized charge distribution across all solvents investigated, which can be likened to Class II mixed-valency.

Applications of solvatochromic complexes and metal-organic frameworks

Potential sensing-based applications of solvatochromic complexes hinge upon a reliable dependence of a measurable parameter (usually λ_{max}) on the quantity to be observed. For example, further investigations on **25** tested its ability to report on the composition of mixed-solvent systems.[20] The excitation wavelength λ_{max} exhibits a linear trend as a function of the

percentage (by volume) of ethanol in water, whereas for a DCM/MeOH mixed solvent system, a deviation from linearity was observed at high DCM concentrations, due to preferential solvation by MeOH.

Turning to the solid state, the ability of some metal organic frameworks (MOFs) to change color upon the exchange of guest solvent molecules can be viewed as a subset of the wider category of host-guest phenomena.[126] Although this behavior is different to the solvatochromism of discrete complexes in solution, the word 'solvatochromic' in the sense so far discussed has been equally applied, throughout the literature, to porous MOFs exhibiting a color changing response upon incorporating different solvent guests, either by immersion in solvent, or by exposure to solvent vapours.[101,126–129] These systems bear much potential for applications in vapor sensing and as solvent indicators.

Despite occurring in the solid state, solvatochromism in MOFs can, in many cases, be understood using similar principles to those that apply to solvatochromism in solution. The color change from red to purple upon desolvation of the MOF $\{[Co(L)(m\text{-}BDC)]\cdot DMF\}_n$ (L = *N,N′*-di(pyridin-4-yl)isophthal-amide, *m*-BDC = 1,3-benzenedicarboxylic acid) arises due to the shift of d-d bands to lower energies as hydrogen bonding DMF molecules are replaced by non-hydrogen bonding void space.[130] The increase in band energies caused by hydrogen bonding interactions mirrors the solvatochromic behavior of many examples discussed above. Likewise, hydrogen bonding is responsible for the solvatochromism of the MOF $\{[Co(34pba)_2]\cdot DMF\}_n$ (34pba = 3-(4-pyridyl)-benzoate), which undergoes a reversible color change upon desolvation from light purple to dark purple.[131] Desolvated sampes of the MOF $\{[Co(44pba)_2]\cdot DMF_3\cdot EtOH_{0.25}\cdot H_2O_4\}_n$ (44pba = 4-(4-pyridyl)-benzoate) were able to be resolvated by a wide range of solvents, with the diffuse reflectance spectra of the resolvated compounds indicating a negative solvatochromism.[132] While hydrogen bonding interactions can again be invoked to rationalize this behavior, crystallographic studies on the MeOH-solvated compound revealed that structural changes may also play a role – slight rotations of aromatic rings and small changes in the Co-N/O bond lengths were found to accompany the uptake of MeOH.[133]

Perhaps the most dramatic structural change possible is a crystal-to-amorphous-to-crystal rearrangement. Such a rearrangement, along with concomitant solvatochromism, has been observed for the MOF $\{[Co(NCS)_2(L)]\cdot 2H_2O\cdot CH_3OH\}_n$ (L = tetrakis(4-pyridyloxymethylene)methane).[134] In the absence of MeOH, the compound undergoes a complete loss of crystallinity and the compound changes from pink to blue (Fig. 15). Re-exposure to MeOH results in a rapid color change back to pink and a recovery of crystallinity.

The process occurs solely with MeOH and persists at low MeOH concentrations as well as in gaseous environments, allowing the system to act as a specific and highly sensitive MeOH sensor that functions in both liquid and gaseous environments. In the same vein, a trinuclear framework $\{[Co_3(OBA)_3(PTD)(OH_2)_2]\cdot 2DMA\cdot H_2O\}_n$ (H_2OBA = 4,4′-oxybis(benzoic acid), PTD = 6-(pyridin-4-yl)-1,3,5-triazine-2,4-diamine) was recently reported to act as a specific, sensitive DCM sensor, exhibiting reversible single-crystal-to-single-crystal solvatochromic phenomena on exposure to DCM.[31]

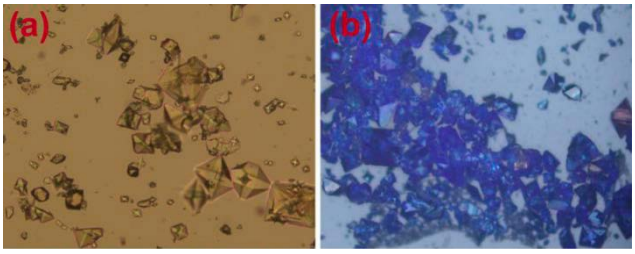

Fig. 15 Color changes in $\{[Co(NCS)_2(L)]\cdot 2H_2O\cdot CH_3OH\}_n$. (a): As synthesized. (b): In the absence of MeOH. Re-exposure to MeOH results in recovery of the characteristic appearance of (a). Adapted with permission from Ref. [134]. Copyright © 2018 American Chemical Society.

Summary and concluding remarks

A tell-tale sign that a suspect compound exhibits valence tautomerism is the observation of a reversible color change upon heating or cooling. Electronic spectroscopy allows us to probe the excitations responsible for these often dramatic effects – the aim of this review has been to illustrate the relationships between optical phenomena and redox isomerism in inorganic molecules. In particular, we have shown that the related phenomena of charge transfer and solvatochromism can provide valuable insights into the switchable behavior, or lack thereof, in a potential VT or CTIST complex.

The relationship between redox isomers is fundamentally tied to the relationship between the ground (D-A) and excited (D^+-A^-) states in a charge transfer excitation. As a consequence, the charge transfer spectra of complexes with two redox-active moieties can indicate, for example, the energy difference between two redox isomers, or whether a particular redox isomer is present under certain conditions, or, by extension, the position of the valence tautomeric equilibrium, if there is one.

In certain systems, the energy of the charge transfer excitation can act as a diagnostic criterion for whether the redox isomers are close enough in energy to observe an equilibrium

between them. As E_{op} is lowered from **1** to **2**, and likewise from **10** to **11**, the D^{+}-A^{-} isomers that were inaccessible in **1** and **10** become present in the room temperature equilibria of **2** and **11**. Accordingly, one might hope to find a certain threshold value of E_{op}, below which redox isomerism is observed, and above which it is not. Indeed, in putative VT systems, it has been proposed that values of the separation between the redox potentials of the frontier metal and ligand redox processes can be used to predict the likelihood of thermal VT interconversion.[23] However, the widely varying charge transfer band energies exhibited by **1** to **17** clearly indicate that no general rule for E_{op} exists. Between different metals and ligand families, the reorganizational energy λ may vary greatly, and so, E_{op} and ΔG_0 are not expected to move in parallel. Additionally, even if a low E_{op} value could be used to imply a close separation of isomers, the accessibility of the transition would still be subject to a favorable entropy difference, which could also vary greatly between different metals and ligand families. Hence, values of E_{op} should only be compared between structurally related systems, for example, between complexes **10** to **13**.

Charge transfer phenomena often come hand-in-hand with solvatochromism. Aside from the related proposed applications in sensing, solvatochromism can also provide a window into a molecule's interactions with its environment. The analysis of solvatochromic trends with solvatochromic parameters can elucidate the nature of solvent-solute interactions, for example, in the case of **23**, where the correlation of ν_{max} with solvent acceptor number suggested that solvation of oxygen atom lone pairs resulted in larger values of Δ_{oct}, or in the case of **25**, where the correlation of λ_{max} with $E_T(30)$ pointed toward hydrogen bonding interactions between solvent and catecholate oxygen atoms.

An understanding of the interpretation of these parameters is critical when drawing conclusions regarding the solvent-solute interactions. For VT systems, such insights could have important ramifications for the solution-state equilibrium – certain interactions could conceivably stabilize one tautomer more than another, and so, the equilibrium could be manipulated by choice of solvent. In our survey of solvent dependent VT equilibria, two prevailing theories emerge: firstly, in many dioxolene complexes of cobalt and other metals, increasing the solvent donor number results in a stabilization of the smaller, low-temperature tautomer. Secondly, in several copper-guanidine systems, increasing the solvent polarity results in a stabilization of the high-temperature tautomer, with DFT calculations confirming, in one case, that this effect is due to the larger dipole moment of the high-temperature tautomer. In several cases, however, the position of the equilibrium correlates neither with donor number nor polarity. Specific solvent-solute interactions, such as hydrogen bonding,

may play an important role, and the effect of the endoergic term (Ω) may be especially relevant to cobalt VT systems.

The discussions outlined above underline the significant effects that solvent-solute interactions can have on molecular behaviors, as well as the importance of investigating behavior in a range of solvents where possible. One of the major barriers to integrating VT molecules into data storage, sensor, or display devices is the possible loss of switchable behavior upon change in environment. Despite pertaining to the solution state, solvatochromic analysis can provide valuable information about the environmental factors that affect VT. These insights may prove useful as ongoing advances approach incorporating switchable molecules into real devices. For example, one novel example of using solution state behaviors to inform solid state properties is found in a study that integrates molecules of complex **42** into liquid-filled microcapsules, which are then incorporated into thin films.[113] The solvatochromism of **42** is used to inform the ideal choice of solvent for the microcapsules, and the VT observed in the solution state is maintained upon incorporation into the solid material.

Part of the attraction of transition metal chemistry lies with the vibrancy and variety of colors that transition metal complexes often exhibit. Optical spectroscopy allows us to quantify these colors. We have discussed herein how the behavior of a compound's spectral bands can illuminate important aspects of its switchability. The response of charge transfer bands to ligand tuning reveals aspects of the relationship between redox isomers, while the response of spectral bands to solvent can reveal environmental effects on redox isomerism. In color, therefore, there exists a wealth of information, the analysis of which can shed light on why a switchable molecule acts the way it does, and thereby inform the design of future switchable molecules, as well as their implementation in the as-yet foreign environment of a molecule-based device.

Biographies

Vincent Nadurata obtained his BSc in chemistry at the University of Melbourne. After a summer research project under Christian Limberg at the Humboldt University of Berlin, he undertook a second undergraduate project under Colette Boskovic, focusing on the synthesis of lanthanoid single-molecule magnets. Continuing with a MSc in the same group, his current research focuses on redox-switchable cobalt complexes.

Colette Boskovic obtained her BSc(Hons) and PhD degrees from the University of Melbourne, undertaking research under the supervision of Tony Wedd. She returned to the University of Melbourne in 2004, where she is now Associate Professor, after postdoctoral positions with George Christou at Indiana University and Hans Güdel at the University of Bern. Her research interests lie in the fields of molecular magnetism, lanthanoid chemistry, polyoxometalate chemistry, redox-active ligands and switchable molecular materials.

References

1 H. B. Li, B. E. Tebikachew, C. Wiberg, K. Moth-Poulsen and J. Hihath, A Memristive Element Based on an Electrically Controlled Single-Molecule Reaction, *Angew. Chem. Int. Ed.*, 2020, **59**, 2–8.

2 J.-F. Létard, P. Guionneau and L. Goux-Capes, "Towards Spin Crossover Applications", *Spin Crossover in Transition Metal Compounds III*, 2006, **1**, 221–249.

3 A. Dei, D. Gatteschi, C. Sangregorio and L. Sorace, Quinonoid metal complexes: Toward molecular switches, *Acc. Chem. Res.*, 2004, **37**, 827–835.

4 Q. Yang, T. Zhong, Z. Tu, L. Zhu, M. Wu and X. C. Zeng, *Adv. Sci.*, Design of Single-Molecule Multiferroics for Efficient Ultrahigh-Density Nonvolatile Memories, 2019, DOI:10.1002/advs.201801572.

5 M. M. Waldrop, More than Moore, *Nature*, 2016, **530**, 144–147.

6 N. Mathur, Beyond the Silicon Roadmap, *Nature*, 2002, **419**, 573–575.

7 J. Conyard, A. Cnossen, W. R. Browne, B. L. Feringa and S. R. Meech, Chemically optimizing operational efficiency of molecular rotary motors, *J. Am. Chem. Soc.*, 2014, **136**, 9692–9700.

8 F. D. Natterer, K. Yang, W. Paul, P. Willke, T. Choi, T. Greber, A. J. Heinrich and C. P. Lutz, Reading and writing single-atom magnets, *Nature*, 2017, **543**, 226–228.

9 D. Shao, L. Shi, F.-X. Shen, X.-Q. Wei, O. Sato and X.-Y. Wang, Reversible On–Off Switching of the Hysteretic Spin Crossover in a Cobalt(II) Complex via Crystal to Crystal Transformation, *Inorg. Chem.*, 2019, **58**, 11589–11598.

10 M. P. Bubnov, K. A. Kozhanov, N. A. Skorodumova and V. K. Cherkasov, Photo- and Thermosensitive Molecular Crystals. Valence Tautomeric Interconversion as the Cause of the Photomechanical Effect in Crystals of Bis(dioxolene)cobalt Complex, *Inorg. Chem.*, 2020, **59**, 6679–6683.

11 T. Tezgerevska, K. G. Alley and C. Boskovic, Valence tautomerism in metal complexes: Stimulated and reversible intramolecular electron transfer between metal centers and organic ligands, *Coord. Chem. Rev.*, 2014, **268**, 23–40.

12 E. Evangelio and D. Ruiz-Molina, Valence tautomerism: More actors than just electroactive ligands and metal ions, *Comptes Rendus Chim.*, 2008, **11**, 1137–1154.

13 C. Benelli, A. Dei, D. Gatteschi and L. Pardi, Redox potentials and charge transfer spectra of catecholate and semiquinone adducts of a cobalt-tetraazamacrocyclic complex, *Inorg. Chim. Acta*, 1989, **163**, 99–104.

14 G. K. Gransbury, B. N. Livesay, J. T. Janetzki, M. A. Hay, R. W. Gable, M. P. Shores, A. Starikova and C. Boskovic, Understanding the Origin of One- or Two-Step Valence Tautomeric Transitions in Bis(dioxolene)-Bridged Dinuclear Cobalt Complexes, *J. Am. Chem. Soc.*, 2020, **142**, 10692–10704.

15 M. M. Zulu and A. J. Lees, Solvent effects on the lowest energy excited states of binuclear $(OC)_5W$-L-$W(CO)_5$ complexes, *Inorg. Chem.*, 1988, **27**, 3325–3331.

16 J. Burgess, J. G. Chambers and R. I. Haines, Structure, solvatochromism, and solvation of trans-$[Co^{III}(cyclam)(NCS)_2](NCS)$ and the structure of $[Co^{II}(Me_4cyclam)(NCS)_2][Co(NCS)_4]MeOH$, *Transit. Met. Chem.*, 1981, **6**, 145–151.

17 S. Barlow, Fe^{II}-to-Co^{III} charge-transfer transitions in methylene-bridged metallocene salts, *Inorg. Chem.*, 2001, **40**, 7047–7053.

18 P. V. Bernhardt, F. Bozoglián, G. González, M. Martínez, B. P. Macpherson and B. Sienra, Tuning the metal-to-metal charge transfer energy of cyano-

bridged dinuclear complexes, *Inorg. Chem.*, 2006, **45**, 74–82.
19 I. Ratera, C. Sporer, D. Ruiz-Molina, N. Ventosa, J. Baggerman, A. M. Brouwer, C. Rovira and J. Veciana, Solvent tuning from normal to inverted marcus region of intramolecular electron transfer in ferrocene-based organic radicals, *J. Am. Chem. Soc.*, 2007, **129**, 6117–6129.
20 G. Cioncoloni, H. M. Senn, S. Sproules, C. Wilson and M. D. Symes, The electronic and solvatochromic properties of $[Co(L)(bipyridine)_2]^+$ (L = o-catecholato, o-benzenedithiolato) species: a combined experimental and computational study, *Dalton Trans.*, 2016, **45**, 15575–15585.
21 C. Reichardt, Solvatochromic Dyes as Solvent Polarity Indicators, *Chem. Rev.*, 1994, **94**, 2319–2358.
22 A. Dei, A. Feis, G. Poneti and L. Sorace, Thermodynamics of valence tautomeric interconversion in a tetrachlorodioxolene:cobalt 1:1 adduct, *Inorg. Chim. Acta*, 2008, **361**, 3842–3846.
23 G. K. Gransbury, M.-E. Boulon, S. Petrie, R. W. Gable, R. J. Mulder, L. Sorace, R. Stranger and C. Boskovic, DFT Prediction and Experimental Investigation of Valence Tautomerism in Cobalt-Dioxolene Complexes, *Inorg. Chem.*, 2019, **58**, 4230–4243.
24 V. Gutmann, Empirical parameters for donor and acceptor properties of solvents, *Electrochim. Acta*, 1976, **21**, 661–670.
25 M. J. Kamlet, J. L. M. Abboud, M. H. Abraham and R. W. Taft, Linear solvation energy relationships. 23. A comprehensive collection of the solvatochromic parameters, π^*, α, and β, and some methods for simplifying the generalized solvatochromic equation, *J. Org. Chem.*, 1983, **48**, 2877–2887.
26 P. G. Jessop, D. A. Jessop, D. Fu and L. Phan, Solvatochromic parameters for solvents of interest in green chemistry, *Green Chem.*, 2012, **14**, 1245.
27 N. Ventosa, D. Ruiz-Molina, J. Sedó, C. Rovira, X. Tomas, J. J. André, A. Bieber and J. Veciana, Influence of the molecular surface characteristics of the diastereoisomers of a quartet molecule on their physicochemical properties: A linear solvation free-energy study, *Chem. Eur. J.*, 1999, **5**, 3533–3548.
28 I. L. Fedushkin, O. V. Maslova, A. G. Morozov, S. Dechert, S. Demeshko and F. Meyer, Genuine redox isomerism in a rare-earth-metal complex, *Angew. Chem. Int. Ed.*, 2012, **51**, 10584–10587.
29 P. Dapporto, A. Dei, G. Poneti and L. Sorace, Complete direct and reverse optically induced valence tautomeric interconversion in a cobalt-dioxolene complex, *Chem. Eur. J.*, 2008, **14**, 10915–10918.
30 Y. Mulyana, G. Poneti, B. Moubaraki, K. S. Murray, B. F. Abrahams, L. Sorace and C. Boskovic, Solvation effects on the valence tautomeric transition of a cobalt complex in the solid state, *Dalton Trans.*, 2010, **39**, 4757–4767.
31 B. Qin, S. Wu, G. Gahungu, H. Li, Y. Zhao, X. Zhang and J. Zhang, A Trinuclear Cobalt–Organic Framework: Solvatochromic Sensor towards CH_2Cl_2, and its Derivative as an Anode of Lithium-Ion Batteries with High Performance, *Chem. Eur. J.*, 2020, **26**, 14187–14193.
32 V. W.-W. Yam, A. K.-W. Chan and E. Y.-H. Hong, Charge-transfer processes in metal complexes enable luminescence and memory functions, *Nat. Rev. Chem.*, 2020, **4**, 528–541.
33 V. Coropceanu, X.-K. Chen, T. Wang, Z. Zheng and J.-L. Brédas, Charge-transfer electronic states in organic solar cells, *Nat. Rev. Mater.*, 2019, **4**, 689–707.
34 K. S. Kjær, N. Kaul, O. Prakash, P. Chábera, N. W. Rosemann, A. Honarfar, O. Gordivska, L. A. Fredin, K.-E. Bergquist, L. Häggström, T. Ericsson, L. Lindh, A. Yartsev, S. Styring, P. Huang, J. Uhlig, J. Bendix, D. Strand, V.

Sundström, P. Persson, R. Lomoth and K. Wärnmark, Luminescence and reactivity of a charge-transfer excited iron complex with nanosecond lifetime, *Science*, 2019, **363**, 249–253.
35 B. S. Brunschwig, C. Creutz and N. Sutin, Optical transitions of symmetrical mixed-valence systems in the class II-III transition regime, *Chem. Soc. Rev.*, 2002, **31**, 168–184.
36 K. G. Alley, G. Poneti, P. S. D. Robinson, A. Nafady, B. Moubaraki, J. B. Aitken, S. C. Drew, C. Ritchie, B. F. Abrahams, R. K. Hocking, K. S. Murray, A. M. Bond, H. H. Harris, L. Sorace and C. Boskovic, Redox activity and two-step valence tautomerism in a family of dinuclear cobalt complexes with a spiroconjugated bis(dioxolene) ligand, *J. Am. Chem. Soc.*, 2013, **135**, 8304–8323.
37 A. Beni, A. Dei, S. Laschi, M. Rizzitano and L. Sorace, Tuning the charge distribution and photoswitchable properties of cobalt-dioxolene complexes by using molecular techniques, *Chem. Eur. J.*, 2008, **14**, 1804–1813.
38 D. M. Adams, B. Li, J. D. Simon and D. N. Hendrickson, Photoinduced Valence Tautomerism in Cobalt Complexes Containing Semiquinone Anion as Ligand: Dynamics of the High-Spin[Co^{II}(3,5-dtbsq)$_2$] to Low-Spin[Co^{III}(3,5-dtbsq)(3,5-dtbcat)] Interconversion, *Angew. Chem. Int. Ed.*, 1995, **34**, 1481–1483.
39 M. Cammarata, S. Zerdane, L. Balducci, G. Azzolina, S. Mazerat, C. Exertier, M. Trabuco, M. Levantino, R. Alonso-Mori, J. M. Glownia, S. Song, L. Catala, T. Mallah, S. F. Matar and E. Collet, Charge transfer driven by ultrafast spin transition in a CoFe Prussian blue analogue, *Nat. Chem.*, 2021, **13**, 10-14.
40 A. Goujon, F. Varret, V. Escax, A. Bleuzen and M. Verdaguer, Thermo-chromism and photo-chromism in a Prussian blue analogue, *Polyhedron*, 2001, **20**, 1339–1345.
41 D. Li, R. Clérac, O. Roubeau, E. Harté, C. Mathonière, R. Le Bris and S. M. Holmes, Magnetic and optical bistability driven by thermally and photoinduced intramolecular electron transfer in a molecular cobalt-iron Prussian blue analogue, *J. Am. Chem. Soc.*, 2008, **130**, 252–258.
42 R. M. Buchanan and C. G. Pierpont, Tautomeric Catecholate-Semiquinone Interconversion via Metal-Ligand Electron Transfer. Structural, Spectral, and Magnetic Properties of (3,5-Di-tert-butylcatecholato)- (3,5-di-tert-butylsemiquinone)(bipyridyl)cobalt(III), a Complex Containing Mixed-Valence Organic Ligands, *J. Am. Chem. Soc.*, 1980, **102**, 4951–4957.
43 M. B. Robin and P. Day, Mixed Valence Chemistry – A Survey and Classification, *Adv. Inorg. Chem. Radiochem.*, 1968, **10**, 247–422.
44 R. Murase, C. F. Leong and D. M. D'Alessandro, Mixed Valency as a Strategy for Achieving Charge Delocalization in Semiconducting and Conducting Framework Materials, *Inorg. Chem.*, 2017, **56**, 14373–14382.
45 M. Biner, H. B. Buergi, A. Ludi and C. Roehr, Crystal and molecular structures of [Ru(bpy)$_3$](PF$_6$)$_3$ and [Ru(bpy)$_3$](PF$_6$)$_2$ at 105 K, *J. Am. Chem. Soc.*, 1992, **114**, 5197–5203.
46 E. S. Koumousi, I. R. Jeon, Q. Gao, P. Dechambenoit, D. N. Woodruff, P. Merzeau, L. Buisson, X. Jia, D. Li, F. Volatron, C. Mathonière and R. Clérac, Metal-to-metal electron transfer in Co/Fe prussian blue molecular analogues: The ultimate miniaturization, *J. Am. Chem. Soc.*, 2014, **136**, 15461–15464.
47 H. J. Buser, A. Ludi, D. Schwarzenbach and W. Petter, The Crystal Structure of Prussian Blue: Fe$_4$[Fe(CN)$_6$]$_3$·xH$_2$O, *Inorg. Chem.*, 1977, **16**, 2704–2710.
48 C. H. Hendon, A. Walsh, N. Akiyama, Y. Konno, T. Kajiwara, T. Ito, H. Kitagawa and K. Sakai, One-dimensional Magnus-type platinum double salts,

Nat. Commun., 2016, **7**, 11950.
49 A. Stebler, J. H. Ammeter, U. Fuerholz and A. Ludi, The Creutz-Taube complex revisited: a single-crystal EPR study, *Inorg. Chem.*, 1984, **23**, 2764–2767.
50 C. Creutz and H. Taube, A Direct Approach to Measuring the Franck-Condon Barrier to Electron Transfer between Metal Ions, *J. Am. Chem. Soc.*, 1969, **91**, 3988–3989.
51 D. M. D'Alessandro and F. R. Keene, Current trends and future challenges in the experimental, theoretical and computational analysis of intervalence charge transfer (IVCT) transitions, *Chem. Soc. Rev.*, 2006, **35**, 424–440.
52 M. P. van Koeverden, B. F. Abrahams, D. M. D'Alessandro, P. W. Doheny, C. Hua, T. A. Hudson, G. N. L. Jameson, K. S. Murray, W. Phonsri, R. Robson and A. L. Sutton, Tuning Charge-State Localization in a Semiconductive Iron(III)–Chloranilate Framework Magnet Using a Redox-Active Cation, *Chem. Mater.*, 2020, **32**, 7551–7563.
53 C. Hassenrück, P. Mücke, J. Scheck, S. Demeshko and R. F. Winter, Oxidized Styrylruthenium–Ferrocene Conjugates: From Valence Localization to Valence Tautomerism, *Eur. J. Inorg. Chem.*, 2017, **2017**, 401–411.
54 H. Petzold, P. Djomgoue, G. Hörner, J. M. Speck, T. Rüffer and D. Schaarschmidt, ^{1}H NMR spectroscopic elucidation in solution of the kinetics and thermodynamics of spin crossover for an exceptionally robust Fe^{2+} complex, *Dalton Trans.*, 2016, **45**, 13798–13809.
55 B. Strauß, V. Gutmann and W. Linert, Spin-crossover complexes in solution, II solvent effects on the high spin-low spin-equilibrium of $[Fe(bzimpy)_2](ClO_4)_2$, *Monatsh. Chem.*, 1993, **124**, 515–522.
56 S. A. Barrett, C. A. Kilner and M. A. Halcrow, Spin-crossover in $[Fe(3\text{-}bpp)_2][BF_4]_2$ in different solvents – A dramatic stabilisation of the low-spin state in water, *Dalton Trans.*, 2011, **40**, 12021.
57 W. Linert, M. Enamullah, V. Gutmann and R. F. Jameson, Spin-crossover complexes in solution. III. Substituent- and solvent effects on the spin-equilibrium of 4-substituted iron(II)-2,6-bis-(benzimidazol-2′-yl)-pyridine systems, *Monatsh. Chem.*, 1994, **125**, 661–670.
58 S. Rodríguez-Jiménez, A. S. Barltrop, N. G. White, H. L. C. Feltham and S. Brooker, Solvent Polarity Predictably Tunes Spin Crossover $T_{1/2}$ in Isomeric Iron(II) Pyrimidine Triazoles, *Inorg. Chem.*, 2018, **57**, 6266–6282.
59 S. Fantacci, F. De Angelis and A. Selloni, Absorption spectrum and solvatochromism of the $[Ru(4,4'\text{-}COOH\text{-}2,2'\text{-}bpy)_2(NCS)_2]$ molecular dye by time dependent density functional theory, *J. Am. Chem. Soc.*, 2003, **125**, 4381–4387.
60 W. Kaim, S. Kohlmann, S. Ernst, B. Olbrich-Deussner, C. Bessenbacher and A. Schulz, What determines the solvatochromism of metal-to-ligand charge transfer transitions? A demonstration involving 17 tungsten carbonyl complexes, *J. Organomet. Chem.*, 1987, **321**, 215–226.
61 I. W. Renk and H. T. Dieck, Zur Komplexchemie von Vierzentren-π-Systemen, V. Die „π-Rückbindung": Solvatochromie bei 1.4-Diheterobutadien-molybdän-tri- und -dicarbonylen, *Chem. Ber.*, 1972, **105**, 1403–1418.
62 R. W. Balk, D. J. Stufkens and A. Oskam, Bonding properties of $Mo(CO)_4$-$xL(PR_3)x$ (x = 0, 1, 2; L =diazabutadiene, pyridine-2-carbaldehyde imine and 2,2′-bipyridine). Infrared, Electronic Absorption, ^{1}H, ^{13}C and ^{31}P NMR and Resonance Raman Spectra, *Inorg. Chim. Acta*, 1978, **28**, 133–143.
63 R. Mitsuhashi, T. Suzuki, Y. Sunatsuki and M. Kojima, Hydrogen-bonding interactions, geometrical selectivity and spectroscopic properties of cobalt(III)

complexes with unsymmetrical tridentate amine-amidato-phenolato type ligands, *Inorg. Chim. Acta*, 2013, **399**, 131–137.
64 R. Warratz, G. Peters, F. Studt, R. H. Römer and F. Tuczek, Orbital interactions in Fe(II)/Co(III) heterobimetallocenes: Single versus double bridge, *Inorg. Chem.*, 2006, **45**, 2531–2542.
65 D. Chatterjee, H. C. Bajaj and A. Das, Synthesis, Kinetics, and Physicochemical Studies of a New Mixed-Valent Heterobinuclear Cyano-Bridged Ruthenium(III)-Iron(II) Complex, *Inorg. Chem.*, 1993, **32**, 4049–4052.
66 J. Guasch, L. Grisanti, S. Jung, D. Morales, G. D'Avino, M. Souto, X. Fontrodona, A. Painelli, F. Renz, I. Ratera and J. Veciana, Bistability of Fc-PTM-Based dyads: The role of the donor strength, *Chem. Mater.*, 2013, **25**, 808–814.
67 T. Mibu, Y. Suenaga, T. Okubo, M. Maekawa and T. Kuroda-Sowa, Spectroscopic characterization of valence tautomeric behavior in a cobalt-dioxolene complex using an ancillary ligand containing quinoline groups, *Inorg. Chem. Commun.*, 2020, **114**, 107826.
68 L. Schnaubelt, H. Petzold, J. M. Speck, T. Rüffer, G. Hörner and H. Lang, Spin Transition and Charge Transfer in Co^{2+}/Co^{3+} Complexes of Meridional Ligands Holding Nearby Redox-active Triarylamine, *Z. Anorg. Allg. Chem.*, 2018, **644**, 1257–1267.
69 L. Schnaubelt, H. Petzold, G. Hörner, T. Rüffer, N. Klein and H. Lang, Tailoring of the Frontier Orbital Character in $Co^{2+/3+}$ Complexes with Triarylamine Substituted Terpyridine Ligands, *Eur. J. Inorg. Chem.*, 2019, **2019**, 988–1001.
70 A. Kochem, H. Kanso, B. Baptiste, H. Arora, C. Philouze, O. Jarjayes, H. Vezin, D. Luneau, M. Orio and F. Thomas, Ligand contributions to the electronic structures of the oxidized cobalt(II) salen complexes, *Inorg. Chem.*, 2012, **51**, 10557–10571.
71 M. Nihei, Y. Sekine, N. Suganami, K. Nakazawa, A. Nakao, H. Nakao, Y. Murakami and H. Oshio, Controlled intramolecular electron transfers in cyanide-bridged molecular squares by chemical modifications and external stimuli, *J. Am. Chem. Soc.*, 2011, **133**, 3592–3600.
72 Y. Dong and J. T. Hupp, Thermochromic Effects in an Asymmetric Mixed-Valence System, *Inorg. Chem.*, 1992, **31**, 3322–3324.
73 O. S. Jung, D. H. Jo, Y. A. Lee, Y. S. Sohn and C. G. Pierpont, Chelate-Ring-Dependent Shifts in Redox Isomerism for the $CoMe_2N(CH_2)_nNMe_2(3,6\text{-}DBQ)_2$ (n = 1-3) Series, Where 3,6-DBQ Is the Semiquinonate or Catecholate Ligand Derived from 3,6-Di-tert-butyl-1,2-benzoquinone, *Inorg. Chem.*, 1998, **37**, 5875–5880.
74 O. S. Jung and C. G. Pierpont, Low-Energy Cobalt(III)-Catechol Electron Transfer. Subtle Coligand Bonding Effects for Co^{III}(N-N)(3,6-DBSQ)(3,6-DBCat) (N-N = 1,10-Phenanthroline, 5-Nitro-1,10-phenanthroline; DBSQ = Di-tert-butylsemiquinonato; DBCat = Di-tert-butylcatecholato), *J. Am. Chem. Soc.*, 1994, **116**, 1127–1128.
75 C. Fleming, D. Chung, S. Ponce, D. J. R. Brook, J. Daros, R. Das, A. Ozarowski and S. A. Stoian, Valence tautomerism in a cobalt-verdazyl coordination compound, *Chem. Commun.*, 2020, **56**, 4400–4403.
76 I. Ratera, D. Ruiz-Molina, F. Renz, J. Ensling, K. Wurst, C. Rovira, P. Gütlich and J. Veciana, A new valence tautomerism example in an electroactive ferrocene substituted triphenylmethyl radical, *J. Am. Chem. Soc.*, 2003, **125**, 1462–1463.
77 G. D'Avino, L. Grisanti, A. Painelli, J. Guasch, I. Ratera and J. Veciana, Cooperativity from electrostatic interactions: understanding bistability in

molecular crystals, *CrystEngComm*, 2009, **11**, 2040–2047.
78 G. D'Avino, L. Grisanti, J. Guasch, I. Ratera, J. Veciana and A. Painelli, Bistability in Fc-PTM crystals: The role of intermodular electrostatic interactions, *J. Am. Chem. Soc.*, 2008, **130**, 12064–12072.
79 D. M. Adams, A. Dei, A. L. Rheingold and D. N. Hendrickson, Bistability in the [Co^{II}(semiquinonate)$_2$] to [Co^{III}(catecholate)(semiquinonate)] valence-tautomeric conversion, *J. Am. Chem. Soc.*, 1993, **115**, 8221–8229.
80 R. Ash, K. Zhang and J. Vura-Weis, Photoinduced valence tautomerism of a cobalt-dioxolene complex revealed with femtosecond M-edge XANES, *J. Chem. Phys.*, 2019, DOI:10.1063/1.5115227.
81 P. Tourón Touceda, S. Mosquera Vázquez, M. Lima, A. Lapini, F. Paolo, D. Andrea and R. Roberto, Transient infrared spectroscopy: A new approach to investigate valence tautomerism, *Phys. Chem. Chem. Phys.*, 2012, **14**, 1038–1047.
82 A. Tashiro, S. Kanegawa, O. Sato and Y. Teki, ESR study of light-induced valence tautomerism of a Co mononuclear complex: [Co(phen)(3,5-DTBSQ)(3,5-DTBCat)], *Polyhedron*, 2013, **66**, 167–170.
83 Y. Teki, M. Shirokoshi, S. Kanegawa and O. Sato, ESR study of light-induced valence tautomerism of a dinuclear Co complex, *Eur. J. Inorg. Chem.*, 2011, **2**, 3761–3767.
84 D. Sato, Y. Shiota, G. Juhász and K. Yoshizawa, Theoretical study of the mechanism of valence tautomerism in cobalt complexes, *J. Phys. Chem. A*, 2010, **114**, 12928–12935.
85 O. S. Jung and C. G. Pierpont, Bistability and Low-Energy Electron Transfer in Cobalt Complexes Containing Catecholate and Semiquinone Ligands, *Inorg. Chem.*, 1994, **33**, 2227–2235.
86 L. Schnaubelt, H. Petzold, E. Dmitrieva, M. Rosenkranz and H. Lang, A solvent- and temperature-dependent intramolecular equilibrium of diamagnetic and paramagnetic states in Co complexes bearing triaryl amines, *Dalton Trans.*, 2018, **47**, 13180–13189.
87 C. T. Cohen, C. M. Thomas, K. L. Peretti, E. B. Lobkovsky and G. W. Coates, Copolymerization of cyclohexene oxide and carbon dioxide using (salen)Co(III) complexes: synthesis and characterization of syndiotactic poly(cyclohexene carbonate), *Dalton Trans.*, 2006, **60**, 237–249.
88 D. D. Ford, L. P. C. Nielsen, S. J. Zuend, C. B. Musgrave and E. N. Jacobsen, Mechanistic Basis for High Stereoselectivity and Broad Substrate Scope in the (salen)Co(III)-Catalyzed Hydrolytic Kinetic Resolution, *J. Am. Chem. Soc.*, 2013, **135**, 15595–15608.
89 W. Kaminsky, A. Funck and H. Hähnsen, New application for metallocene catalysts in olefin polymerization, *Dalton Trans.*, 2009, 8803.
90 T. Kurahashi and H. Fujii, Unique ligand-radical character of an activated cobalt salen catalyst that is generated by aerobic oxidation of a cobalt(II) salen complex, *Inorg. Chem.*, 2013, **52**, 3908–3919.
91 O. Sato, Y. Einaga, T. Iyoda, A. Fujishima and K. Hashimoto, Cation-Driven Electron Transfer Involving a Spin Transition at Room Temperature in a Cobalt Iron Cyanide Thin Film, *J. Phys. Chem. B*, 1997, **101**, 3903–3905.
92 D. Aguilà, Y. Prado, E. S. Koumousi, C. Mathonière and R. Clérac, Switchable Fe/Co Prussian blue networks and molecular analogues, *Chem. Soc. Rev.*, 2016, **45**, 203–224.
93 E. Wagner-Czauderna, A. Boroń-Cegiełkowska, E. Orłowska and M. K. Kalinowski, Solvatochromic equilibria of cobalt(II) chloride in binary mixtures of dipolar aprotic solvents with water, *Transit. Met. Chem.*, 2004, **29**, 61–65.

94 Y. Song, C. Massera, G. A. van Albada, A. M. M. Lanfredi and J. Reedijk, Synthesis, structural characterisation and solvatochromism of a Ni(II) and a Co(II) compound with 2-aminopyrimidine as a ligand, *J. Mol. Struct.*, 2005, **734**, 83–88.

95 M. Amirnasr, V. Langer, N. Rasouli, M. Salehi and S. Meghdadi, Synthesis, characterization, and single crystal X-ray structures of $[Co^{III}(acacen)(thioacetamide)_2]ClO_4$ and $[Co^{III}((BA)_2en)(thioacetamide)_2]PF_6$ - Solvatochromic properties of $[Co^{III}(acacen)(thioacetamide)_2]ClO_4$, *Can. J. Chem.*, 2005, **83**, 2073–2081.

96 M. Salehi, M. Amirnasr and K. Mereiter, Synthesis, characterization, solvatochromic behavior and crystal structures of complexes $[Co^{III}(salophen)(thioacetamide)_2]ClO_4$ and $[Co^{III}(salophen)(thiobenzamide)_2]ClO_4$, *J. Iran. Chem. Soc.*, 2010, **7**, 740–751.

97 M. Salehi, M. Amirnasr and K. Mereiter, Synthesis, characterization, and single crystal X-ray structures of $[Co^{III}((BA)_2en)(thiobenzamide)_2]PF_6$ and $[Co^{III}(acacen)(thiobenzamide)_2]ClO_4$ and their solvatochromic properties, *Transit. Met. Chem.*, 2009, **34**, 373–381.

98 M. Lalia-Kantouri, C. D. Papadopoulos, M. Quirós and A. G. Hatzidimitriou, Synthesis and characterization of new Co(III) mixed-ligand complexes, containing 2-hydroxy-aryloximes and α-diimines. Crystal and molecular structure of $[Co(saox)(bipy)_2]Br$, *Polyhedron*, 2007, **26**, 1292–1302.

99 M. Fujiwara, M. Yoshitake, Y. Fukuda and K. Sone, Solvatochromism of the Co(III) complexes with macrocyclic N_3O_3-type ligands, *Bull. Chem. Soc. Jpn.*, 1988, 61, 2967–2968.

100 R. Mitsuhashi, T. Suzuki, Y. Sunatsuki and M. Kojima, Hydrogen-bonding interactions, geometrical selectivity and spectroscopic properties of cobalt(III) complexes with unsymmetrical tridentate amine-amidato-phenolato type ligands, *Chem. Lett.*, 2011, **40**, 696–698.

101 T. Tezgerevska, E. Rousset, R. W. Gable, G. N. L. Jameson, E. C. Sañudo, A. Starikova and C. Boskovic, Valence tautomerism and spin crossover in pyridinophane–cobalt–dioxolene complexes: an experimental and computational study, *Dalton Trans.*, 2019, **48**, 11674–11689.

102 S. Jeon, H. Lee, H. K. Lee, Y.-K. Choi and O.-S. Jung, Redox Chemistry and Valence Tautomerism of Cobalt-Quinone Complees in Nonaqueous Solvents, *Bull. Korean Chem. Soc.*, 1998, **19**, 212–217.

103 O. S. Jung, D. H. Jo, Y. A. Lee, B. J. Conklin and C. G. Pierpont, Bistability and Molecular Switching for Semiquinone and Catechol Complexes of Cobalt. Studies on Redox Isomerism for the Bis(pyridine) Ether Series $Co(py_2X)(3,6\text{-}DBQ)_2$, X = O, S, Se, and Te, *Inorg. Chem.*, 1997, **36**, 19–24.

104 A. Caneschi and A. Dei, Valence Tautomerism in a o-Benzoquinone Adduct of a Tetraazamacrocycle Complex of Manganese, *Angew. Chem. Int. Ed.*, 1998, **37**, 3005–3007.

105 I. Ando, T. Fukuishi, K. Ujimoto and H. Kurihara, Oxidation states and redox behavior of ruthenium ammine complexes with redox-active dioxolene ligands, *Inorg. Chim. Acta*, 2012, **390**, 47–52.

106 A. Dei, Correlations between Optical Charge Transfer Energies and Electrochemical Data: The Iron (III)-Catecholato System, *Inorg. Chem.*, 1993, **32**, 5730–5733.

107 A. S. Attia, S. Bhattacharya and C. G. Pierpont, Potential for Redox Isomerism by Quinone Complexes of Iron(III). Studies on Complexes of the Fe^{III}(N-N)(DBSQ)(DBCat) Series with 2,2′-Bipyridine and *N,N,N′,N′*-Tetramethylethylenediamine Coligands, *Inorg. Chem.*, 1995, **34**, 4427–4433.

108 S. Wiesner, A. Wagner, E. Kaifer and H. J. Himmel, A Valence Tautomeric Dinuclear Copper Tetrakisguanidine Complex, *Chem. Eur. J.*, 2016, **22**, 10438–10445.
109 D. F. Schrempp, E. Kaifer, H. Wadepohl and H. J. Himmel, Copper Complexes of New Redox-Active 4,5-Bisguanidino-Substituted Benzodioxole Ligands: Control of the Electronic Structure by Counter-Ligands, Solvent, and Temperature, *Chem. Eur. J.*, 2016, **22**, 16187–16199.
110 H. Liang, Y. M. Na, I. S. Chun, S. S. Kwon, Y. A. Lee and O. S. Jung, Dinuclear valence tautomeric 1,2-semiquinonato/catecholatoeobalt complexes containing 1,1,4,7,10,10-hexamethyltriethylenetetramine, *Bull. Chem. Soc. Jpn.*, 2007, **80**, 916–921.
111 A. S. Attia, O. S. Junga and C. G. Pierpont, Valence tautomerism for catechol/semiquinone complexes of the trans-$M(Bupy)_2(3,6\text{-}DBQ)_2$ (M = Mn, Fe, Co) series, *Inorg. Chim. Acta*, 1994, **226**, 91–98.
112 M. Mörtel, M. Seller, F. W. Heinemann and M. M. Khusniyarov, A valence tautomeric cobalt–dioxolene complex with an anchoring group for prospective chemical grafting to metal oxides, *Dalton Trans.*, 2020, **49**, 17532–17536.
113 N. A. Vázquez-Mera, C. Roscini, J. Hernando and D. Ruiz-Molina, Liquid-Filled Valence Tautomeric Microcapsules: A Solid Material with Solution-Like Behavior, *Adv. Funct. Mater.*, 2015, **25**, 4129–4134.
114 N. Shaikh, S. Goswami, A. Panja, X. Y. Wang, S. Gao, R. J. Butcher and P. Banerjee, New route to the mixed valence semiquinone-catecholate based mononuclear Fe^{III} and catecholate based dinuclear Mn^{III} complexes: First experimental evidence of valence tautomerism in an iron complex, *Inorg. Chem.*, 2004, **43**, 5908–5918.
115 E. Evangelio, C. Rodriguez-Blanco, Y. Coppel, D. N. Hendrickson, J. P. Sutter, J. Campo and D. Ruiz-Molina, Solvent effects on valence tautomerism: A comparison between the interconversion in solution and solid state, *Solid State Sci.*, 2009, **11**, 793–800.
116 H. Huesmann, C. Förster, D. Siebler, T. Gasi and K. Heinze, Amide-Linked Heterobi- and Heterotermetallocenes with Very Low HOMO–LUMO Gaps, *Organometallics*, 2012, **31**, 413–427.
117 M. W. Lynch, D. N. Hendrickson, B. J. Fitzgerald and C. G. Pierpont, Intramolecular Two-Electron Transfer between Manganese(II) and Semiquinone Ligands. Synthesis and Characterization of Manganese 3,5-Di-tert-butylquinone Complexes and Their Relationship to the Photosynthetic Water Oxidation System, *J. Am. Chem. Soc.*, 1984, **106**, 2041–2049.
118 N. Kundu, M. Maity, P. B. Chatterjee, S. J. Teat, A. Endo and M. Chaudhury, Reporting a unique example of electronic bistability observed in the form of valence tautomerism with a copper(II) helicate of a redox-active nitrogenous heterocyclic ligand, *J. Am. Chem. Soc.*, 2011, **133**, 20104–20107.
119 D. E. Leahy, P. W. Carr, R. S. Pearlman, R. W. Taft and M. J. Kamlet, Linear solvation energy relationships. A comparison of molar volume and intrinsic molecular volume as measures of the cavity term in reversed phase liquid chromatography, *Chromatographia*, 1986, **21**, 473–477.
120 F. Delgado-Pena, D. R. Talham and D. O. Cowan, Near-IR spectroscopic studies of mixed-valence di-, tri-, and tetraferrocene derivatives, *J. Organomet. Chem.*, 1983, **253**, C43–C46.
121 P. V. Bernhardt, F. Bozoglián, B. P. Macpherson and M. Martínez, Molecular mixed-valence cyanide bridged Co^{III}-Fe^{II} complexes, *Coord. Chem. Rev.*, 2005, **249**, 1902–1916.
122 P. V. Bernhardt, F. Bozoglian, B. P. Macpherson and M. Martinez, Tuning the

metal-to-metal charge transfer energy of cyano-bridged dinuclear complexes, *Dalton Trans.*, 2004, 2582–2587.
123 P. V. Bernhardt, F. Bozoglian, B. P. Macpherson, M. Martínez, G. González and B. Sienra, Discrete cyanide-bridged mixed-valence Co/Fe complexes: Outer-sphere redox behaviour, *Eur. J. Inorg. Chem.*, 2003, 2512–2518.
124 N. S. Hush, Homogeneous and heterogeneous optical and thermal electron transfer, *Electrochim. Acta*, 1968, **13**, 1005–1023.
125 G. C. Allen and N. S. Hush, Intervalence-Transfer Absorption. Part 2. Theoretical Considerations and Spectroscopic Data, in *Progress in Inorganic Chemistry Volume 8*, ed. F. A. Cotton, 1967, pp. 391–444.
126 Z. Z. Lu, R. Zhang, Y. Z. Li, Z. J. Guo and H. G. Zheng, Solvatochromic behavior of a nanotubular metal-organic framework for sensing small molecules, *J. Am. Chem. Soc.*, 2011, **133**, 4172–4174.
127 P. Müller, F. M. Wisser, P. Freund, V. Bon, I. Senkovska and S. Kaskel, Optical Sensors Using Solvatochromic Metal-Organic Frameworks, *Inorg. Chem.*, 2017, **56**, 14164–14169.
128 Z. Cui, X. Zhang, S. Liu, L. Zhou, W. Li and J. Zhang, Anionic Lanthanide Metal-Organic Frameworks: Selective Separation of Cationic Dyes, Solvatochromic Behavior, and Luminescent Sensing of Co(II) Ion, *Inorg. Chem.*, 2018, **57**, 11463–11473.
129 Kirandeep, A. Husain, A. K. Kharwar, R. Kataria and G. Kumar, Co(II)-based Metal-Organic Frameworks and Their Application in Gas Sorption and Solvatochromism, *Cryst. Growth Des.*, 2019, **19**, 1640–1648.
130 Y. Gong, Y. Zhou, J. Li, R. Cao, J. Qin and J. Li, Reversible color changes of metal(II)-N^1,N^3-di(pyridin-4-yl)isophthalamide complexes via desolvation and solvation, *Dalton Trans.*, 2010, **39**, 9923.
131 G. Mehlana, S. A. Bourne, G. Ramon and L. Öhrström, Concomitant Metal Organic Frameworks of Cobalt(II) and 3-(4-Pyridyl)benzoate: Optimized Synthetic Conditions of Solvatochromic and Thermochromic Systems, *Cryst. Growth Des.*, 2013, **13**, 633–644.
132 G. Mehlana, S. A. Bourne and G. Ramon, A new class of thermo- and solvatochromic metal–organic frameworks based on 4-(pyridin-4-yl)benzoic acid, *Dalton Trans.*, 2012, **41**, 4224.
133 G. Mehlana, G. Ramon and S. A. Bourne, Methanol mediated crystal transformations in a solvatochromic metal organic framework constructed from Co(II) and 4-(4-pyridyl) benzoate, *CrystEngComm*, 2013, **15**, 9521.
134 P. Hu, L. Yin, A. Kirchon, J. Li, B. Li, Z. Wang, Z. Ouyang, T. Zhang and H. C. Zhou, Magnetic Metal-Organic Framework Exhibiting Quick and Selective Solvatochromic Behavior along with Reversible Crystal-to-Amorphous-to-Crystal Transformation, *Inorg. Chem.*, 2018, **57**, 7006–7014.

Table of Contents entry

Solvent-induced color-changing phenomena exhibited by some metal complexes can illuminate key aspects of their switchable behavior.